6-13-2018 9:30 AM

Circannual Patterns of Adipose Tissue Characteristics in a Hibernator, the Thirteen-lined Ground Squirrel (Ictidomys tridecemlineatus)

Amanda Maccannell
The University of Western Ontario

Supervisor
Staples, James F.
The University of Western Ontario Joint Supervisor
McKenzie, Charles A.
The University of Western Ontario

Graduate Program in Biology
A thesis submitted in partial fulfillment of the requirements for the degree in Master of Science

Circannual patterns of adipose tissue characteristics in a hibernator, the thirteen-lined ground squirrel (*Ictidomys tridecemlineatus)*

Abstract

Obligate hibernators express circannual patterns of body mass and hibernation, which persist under constant laboratory conditions. I hypothesized that in the 13-lined ground squirrel (*Ictidomys tridecemlineatus*) thermogenic brown adipose tissue (BAT) and lipid storing white adipose tissue (WAT) volume would follow a circannual pattern. I housed animals at either 25°C (thermoneutral) or 5°C with 12h L:12h D photoperiods for an entire year. I determined volume and water-fat ratio of WAT and BAT using magnetic resonance imaging (MRI). BAT volume follows a circannual pattern in both conditions, increasing prior to winter, decreasing in late winter with no change in water-fat ratio. Both body mass and WAT volume of cold-housed animals declined throughout the winter and recovered after hibernation. By contrast, thermoneutral housing produced no circannual pattern in body mass even though WAT volume declined in late winter. Warm-housed animals never entered torpor indicating that they might not be obligate hibernators.

Keywords

white adipose tissue, brown adipose tissue, endogenous circannual rhythm, proton density fat fraction, hibernation, 13-lined ground squirrel

Co-Authorship Statement

Experiments involved in the endogenous rhythms of adipose tissue project (Chapters 3.1, 3.2, 3.3 (figures 3.5, 3.6, 3.7 and 3.8)) (Environmental Temperature Effects on Adipose Tissue Growth in a Hibernator) is in preparation for submission to the *Journal of Experimental Biology* with Kevin J. Sinclair, Dr. Charles A. McKenzie and Dr. James F. Staples as co-authors. Sinclair assisted with MRI data collection. Dr. McKenzie and Dr. Staples contributed to experimental design and provided editorial input. I contributed to experimental design, performed the experiments, analyzed the data, and wrote the manuscript.

Experiments involved in the orbital lipid depot project (Chapter 3.3, figures 3.9, 3.10 and 3.11) (Identification of a lipid rich depot in the orbital cavity of the 13-lined ground squirrel) is in preparation for submission to the *Journal of Experimental Biology* as a short communication with Dr. Charles A. McKenzie and Dr. James F. Staples as co-authors. Dr. McKenzie and Dr. Staples contributed to experimental design and provided editorial input. I contributed to experimental design, performed the experiments, analyzed the data, and wrote the manuscript.

Acknowledgments

There are many people I would like to thank for their support in helping me to achieve my MSc.

First and foremost, my two supervisors: Drs. Staples and McKenzie, for their mentorship and encouragement throughout my time as a Masters student; Dr. Staples for encouraging me to improve my writing skills and for believing in my potential and Dr. McKenzie for his pep talks and immense patience. I am grateful to have had the opportunity to learn so much from both of you.

To my lab mates from both the Staples and McKenzie labs - for the mandatory lab fun and board game afternoons that got me through the long weeks. You all really made my time in graduate school enjoyable and successful.

To my advisors Drs Guglielmo and Sinclair for their guidance and support- it kept me on track and gave me many invaluable ideas.

For the many collaborators that it took to make this project come together: Dr. Glenn Tattersall for use of his thermal camera; Dr. Manujendra Saha for teaching me how to do immunoblots; Dr. Robert Cumming for use of gel imager; Prasiddha Parthasarathy for being a second reader on my MRIs; Dr. Kate Mathers, Leah Hayward, Miya Wang and Sharla Thompson for their endless animal care help.

Finally, I would like to thank my friends and family for unfailing emotional support and continuous encouragement.

Table of Contents

List of Figures

List of Appendices

List of Abbreviations and Symbols

ADP	adenosine 5’-diphosphate
BAT	brown adipose tissue
BSA	bovine serum albumin
D	dark
DTNB	5,5'-Dithiobis(2-nitrobenzoic acid)
EDTA	ethylenediaminetetraacetic acid
ETS	electron transport system
^{1}H	hydrogen proton
H&E	hematoxylin and eosin
HEPES	4-2(2-hydroxyethyl)-1-piperazineethanesulfonic acid
IBE	interbout euthermia
IDEAL	Iterative Decomposition of water and fat with Echo Asymmetry and Least-squares estimation
L	light
MRI	magnetic resonance imaging
PECAM-1	platelet endothelial cell adhesion molecule
PDFF	proton density fat fraction
RIPA	radioimmunoprecipitation assay buffer
SDS	sodium dodecyl sulfate
SCN	suprachiasmatic nucleus
TAG	triacylglycerol
TBST	tris-buffered saline and Tween-20

Ta	ambient temperature
Tb	core body temperature
TE	echo time
TR	relaxation time
UCP1	uncoupling protein-1
UCP3	uncoupling protein-3
VCAM-1	vascular cell adhesion molecule 1
WAT	white adipose tissue

Chapter 1

1 Introduction

Mammals typically maintain a constant core body temperature (T_b) regardless of changes to ambient temperature (T_a). Small endotherms, such as ground squirrels, can be challenged at cold T_a because of the enormous amounts of metabolic energy required to maintain a constant T_b in the cold. Some small endotherms have adapted a life history strategy to this challenge by undergoing seasonal hibernation (Humphries et al., 2003). Hibernation can be classified as obligate, wherein hibernation occurs regardless of environmental conditions, or facultative, in which case exposure to several days of reduced T_a is required to elicit the hibernation phenotype (Strijkstra, 2009). Obligate hibernators display circannual patterns of mass and hibernation which persist under constant laboratory conditions, suggesting they are regulated by endogenous rhythms (Pengelley and Asmundson, 1969).

1.1 Thermal strategies

Homeothermic endotherms are animals that maintain a constant T_b by producing metabolic heat. Maintenance of T_b higher than T_a increases energy expenditure and can be challenging for small homeothermic endotherms in the winter when temperatures are low and food resources are scarce (Humphries et al., 2003). Endotherms can avoid decreases in T_a by migrating to escape the harsh environments. For those that do not migrate, there are some thermoregulatory strategies that small mammals use in an attempt to maintain higher T_b than T_a to minimize energy expenditure. Fur and feathers can provide thermal insulation by their own physical properties, but also by trapping a layer of air around an animal (Scholander et al., 1950). Air trapped between either feathers or fur can be warmed with body heat, and because the air is stagnant and itself a poor thermal conductor, this layer provides further insulation (Scholander et al., 1950). Piloerection aids in this phenomenon by causing hairs to stand on end and trapping more air (Herrington, 1951). Fat located below the skin acts as an additional insulator because fat does not conduct heat as well as muscle or skin. Fat can also be used for additional

metabolic energy storage (Trayhurn and Beattie, 2001).

Physiological and anatomical changes to blood flow can retain or re-direct heat. Vasoconstriction reduces blood flow to tissues immediately below the skin to reduce heat loss across the skin. Another mechanism is countercurrent heat exchange, which can reduce heat lost at extremities by exchanging heat from warm blood in vessels moving toward the periphery of the body with cooler blood returning in vessels from the extremities. For example, the Arctic fox (*Vulpes lagopus*) has counter-current heat exchange between arteries and veins in the limbs which frequently come into contact with sub-zero temperatures through walking on ice and snow (Henshaw et al., 1972). If these mechanisms of heat retention are insufficient to maintain T_b, endotherms must increase metabolic heat production by using both shivering or non-shivering thermogenesis.

Some small mammals have adapted differently to the thermal and energetic challenges of winter by undergoing seasonal hibernation, a strategy that is characterized by bouts of torpor that are interrupted by periods of interbout euthermia (IBE). During entrance into a torpor bout Richardson's ground squirrels (*Urocitellus richardsonii*) show, whole-animal metabolic rate, heart rate and T_b are suppressed by 90%, 100-fold, and 32°C, respectively (Wang, 1979). Hibernation is either facultative, in which hibernation only occurs under specific environmental conditions that typify the onset of winter, or obligate, in which hibernation occurs at approximately the same time each year regardless of environmental conditions (Strijkstra, 2009). Facultative hibernators include the Syrian hamster, which only hibernates after acclimation for approximately 74 days to cold T_a (5°C) and short (8h Light (L):16h Dark (D)) photoperiods (Chayama et al., 2016). Obligate hibernation is thought to be regulated by an endogenous circannual rhythm (see section 1.2 below) as demonstrated by the golden-mantled ground squirrel (*Callospermophilus lateralis*). Juvenile golden-mantled ground squirrels housed under constant environmental conditions of 3°C, 12°C and 22°C with a 12h L:12h D photoperiod for more than four years, showed fluctuating patterns of body mass, food intake, fat storage and hibernation with a period of approximately one year, corresponding largely with patterns seen in wild populations (Pengelley and Asmundson, 1969, Florant et al., 2012). These patterns suggest that the endogenous rhythm regulating

obligate hibernation is controlled genetically and not environmentally (Pengelley and Asmundson, 1969).

The 13-lined ground squirrel (*Ictidomys tridecemlineatus*) is a common experimental hibernation model. This species is widely distributed across the prairies and grasslands of North America and ranges from central Canada to the southern United States. The 13-lined ground squirrel hibernates from late autumn to early spring. During the hibernation season periods of torpor with reduced T_b of ~5°C last for 12-14 days before being interrupted by spontaneous arousals to periods of IBE with T_b of ~37°C and lasting for 10-12 hours (Figure 1.1). Hibernation patterns of free-ranging 13-lined ground squirrels closely resembles those of captive conspecifics, with torpor bouts lasting 12-15 days at a T_b of ~5°C and IBE lasting a mean of 12 hours at a T_b of ~37°C (Kisser and Goodwin, 2012) During IBE, metabolic rate, heart rate and T_b recover within a few hours to levels comparable to the summer euthermic state. It has been speculated that the 13-lined ground squirrel is an obligate hibernator based on its close phylogenetic relationship to known obligate hibernators such as the Arctic ground squirrel (Drew et al., 2007, Russell et al., 2010).

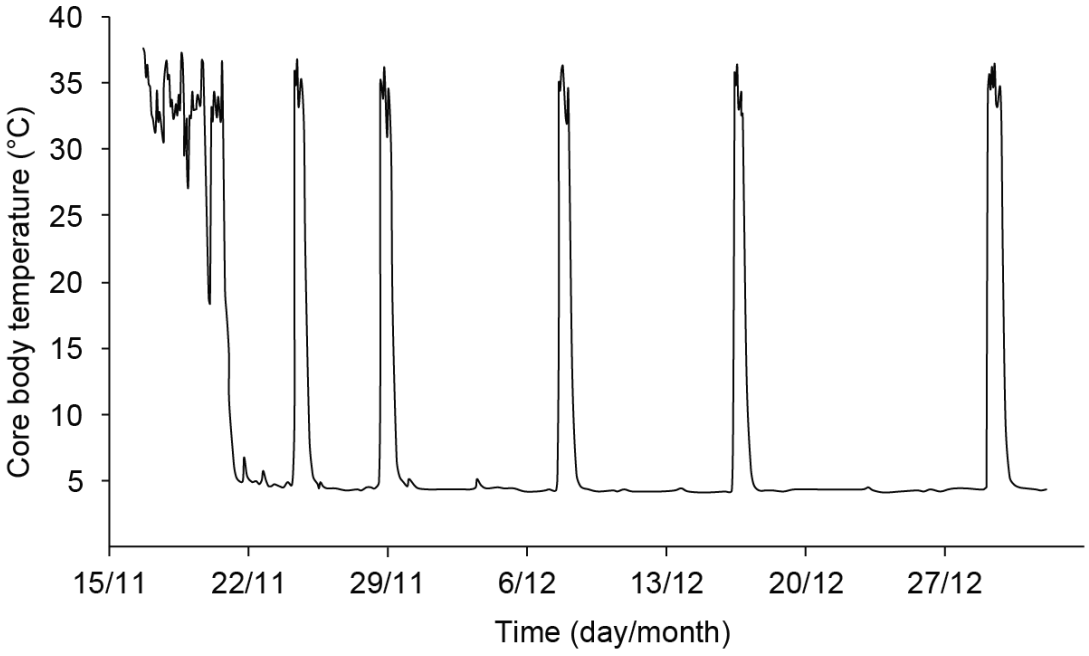

Figure 1.1 Core body temperature (T_b) of a hibernating 13-lined ground squirrel in late autumn and winter. Torpor bouts (where T_b is approximately 5°C) are interrupted by spontaneous arousals to periods of interbout euthermia (T_b ~ 37°C). Tb measurements were made using temperature sensitive radio telemeters implanted intraperitoneally. Modified from Staples (2016).

1.2 Endogenous rhythms

An endogenous rhythm is a periodic biological process which occurs without environmental cues (Aschoff, 1981). Endogenous rhythms offer a potential selective advantage because they allow animals to adjust physiological processes to prepare for predictable environmental changes. Rhythms at the daily scale typically involve endogenously derived oscillations are controlled by "Clock genes" through regulated transcription-translation negative-feedback loops (Hardin et al., 1990, Hardin et al., 1992). Genes found in *Drosophila melanogaster* (*Clock, Bmal1, Period* and *Timeless*) are conserved (homologous) in mammals (*Clock, Bmal1, Period* and *cryptochrome*). All four genes have a role in regulating transcription/translation and therefore creating a circadian endogenous rhythm (Figure 1.2; King and Takahashi, 2000). This process involves one circadian cycle, as the feedback loop takes ~24 hours to complete. This self-oscillating pattern of gene expression allows for the circadian control of physiological properties which include sleep, metabolism and immune responses (Andreani et al., 2015). Circadian rhythms in diurnal rodents are associated with fluctuations in T_b (up to 2-4°C) that coincide with expected photoperiod (Refinetti and Menaker, 1992). Although circadian patterns are self-oscillating, their periods are not exactly 24 hours so they may require an environmental cue, a zeitgeber, to entrain the pattern of gene expression to a 24 hour period (Pittendrigh, 1960).

In mammals the regulation of circadian patterns are controlled by one "master clock": the suprachiasmatic nucleus (SCN), a region in the hypothalamus (Moore 1983 and Moore et al. 2002). The SCN of rodents contains 20,000 neurons and has a near perfect daily rhythm of transcription, translation, metabolism and neuropeptide secretion without environmental cues (Herzog, 2007, Maywood et al., 2006). The cells within this "master clock" entrain and control the negative-feedback loop located within other cells in the body.

Not all endogenous rhythms have a 24-hour period. For example, lunar and semi-diurnal patterns are widely observed in tidal species (Hauenschild, 1960). Additionally, circannual rhythms have a period of approximately one year, and are shown to control

mass changes in obligate hibernators (Pengelley and Asmundson, 1969). The mechanisms that control circannual endogenous rhythms are distinct from those regulating circadian rhythms. Ablation of the SCN in golden-mantled ground squirrels affected all circadian rhythms, but only affected the circannual rhythm of body mass gain in 33% of squirrels (Dark et al. 1984). To my knowledge there is no information about the circannual molecular pathway, but circannual rhythms are theorized to be controlled by the pars tuberalis in the pituitary gland (Lincoln et al., 2006). This theory was developed using sheep models and suggests that melatonin-receptor-containing cells in the pituitary gland may operate as “calendar cells” and transmit seasonal information to the endocrine system (Dupré and Loudon, 2007).

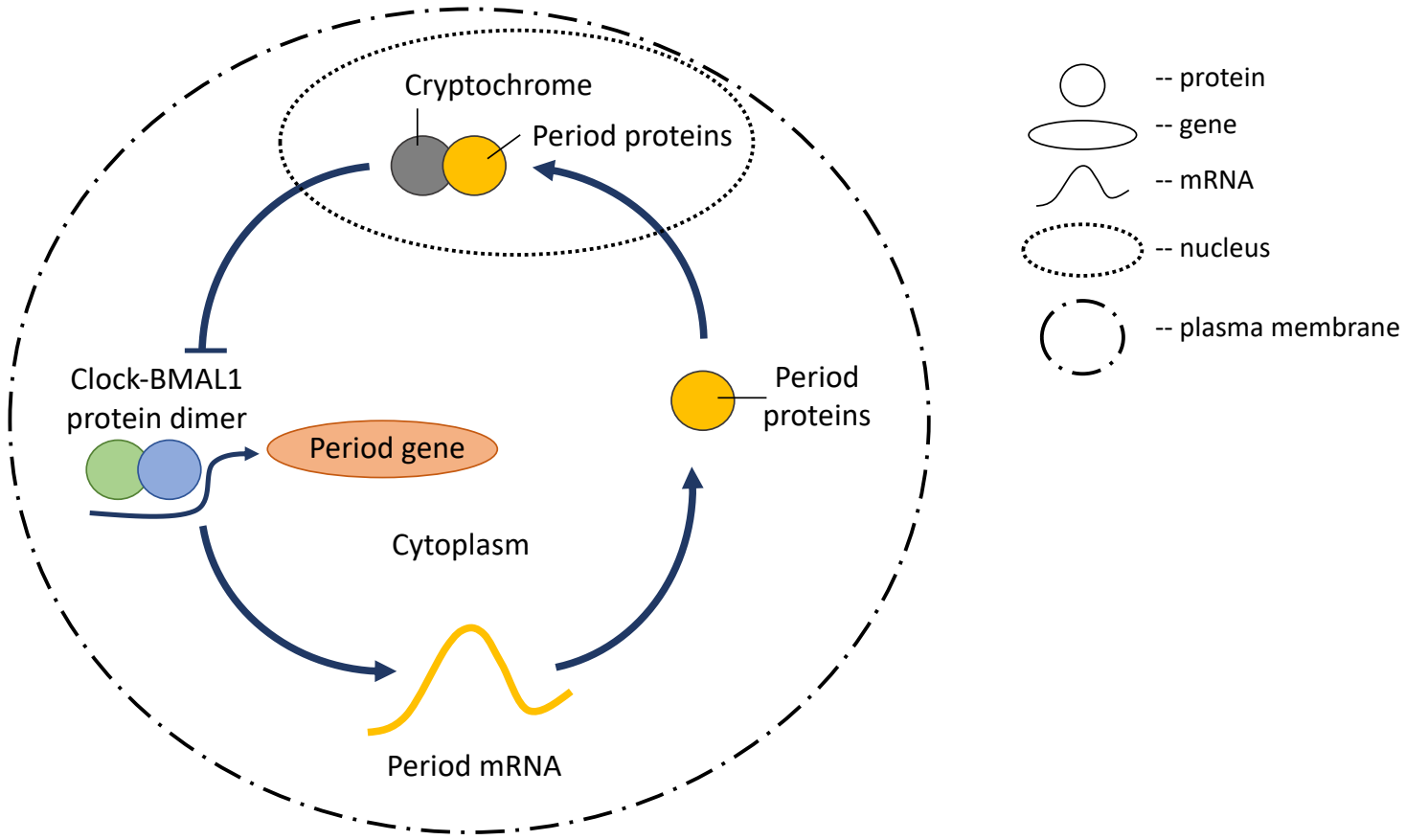

Figure 1.2 An intracellular transcription-translation negative-feedback loop that generates a circadian rhythm. The Clock-BMAL1 protein dimer activates *period* gene transcription to produce *period* mRNA. The Period protein accumulates and translocates into the nucleus and associates with partner proteins (for example, *Cryptochrome* in mammals, or *Timeless* in flies), which repress their own transcription by inhibiting the activity of the Clock-BMAL1 protein dimer. The gradual loss of Period protein leads to de-repression allowing for the daily cycle to start over. Modified from Herzog (2007).

1.3 White adipose tissue

WAT is white/yellowish in color and its adipocytes contain a single large lipid droplet (Figure 1.3). WAT is the primary metabolic energy reserve in mammals, it synthesizes and stores triacylglycerol (TAG) when caloric consumption exceeds expenditure. During periods of negative energy balance, WAT can hydrolyze TAG stores, exporting fatty acids and glycerol for use by other tissues. Beyond storage of metabolic energy, WAT has endocrine functions through its ability to secrete hormones and cytokines (Vázquez-Vela et al., 2008) and can provide thermal insulation and mechanical cushioning for internal organs.

WAT is the main driver of body mass gain prior to hibernation in wild Arctic ground squirrel (*Spermophilus parryii)* (Sheriff et al., 2013) and 13-lined ground squirrels (MacCannell et al., 2017). WAT shows a circannual endogenous rhythm in Artic ground squirrels with depots increasing in size during late summer and early fall in anticipation of winter (Sheriff et al., 2013). Indeed, the pattern of WAT volume change of our captive 13-lined ground squirrels resembled closely that of wild Arctic ground squirrels, with WAT comprising close to 60% of the body volume at its peak in September (MacCannell et al., 2017). The study, however, did not distinguish between subcutaneous and visceral WAT, nor could it evaluate any potential endogenous, circannual rhythm to WAT accumulation.

There are two primary and distinct locations of WAT within mammals: subcutaneous and visceral. Subcutaneous WAT is found below the skin and fat accumulation in this area is the initial storage depot when food energy intake exceeds metabolic energy expenditure (Wronska and Kmiec, 2012). When the storage capacity of the visceral WAT is reached, fat begins to accumulate as subcutaneous WAT outside of the abdomen (Wronska and Kmiec, 2012). Subcutaneous adipose can serve as thermal insulation, and visceral adipose may provide mechanical cushioning for major organs (Wronska and Kmiec, 2012).

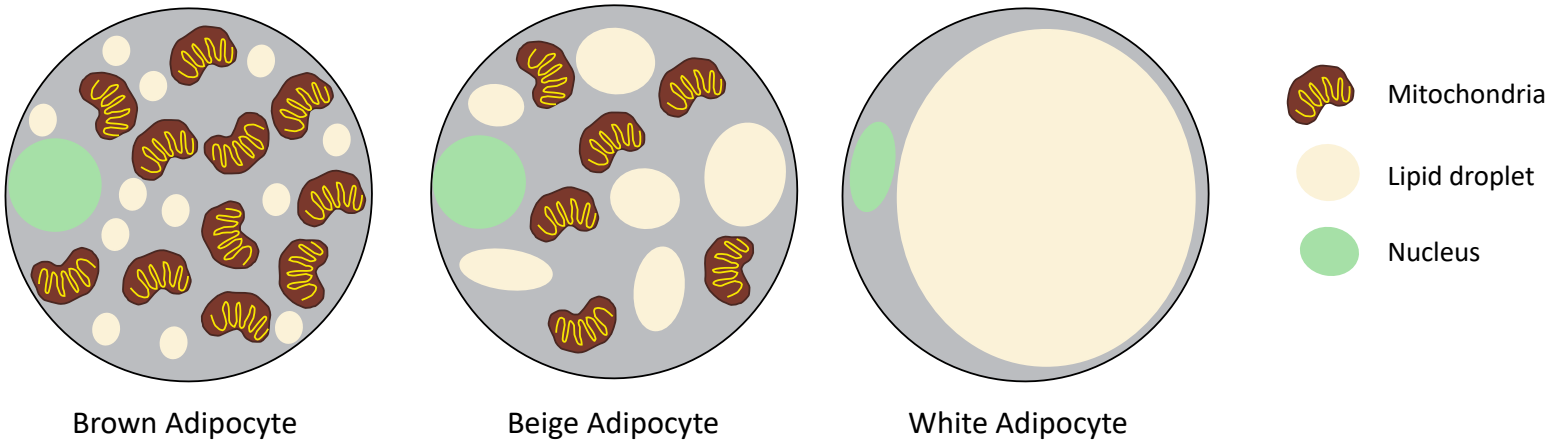

Figure 1.3 Brown, beige and white adipocyte cellular properties. Brown adipocytes contain many mitochondria and multiple small lipid droplets. White adipocytes contain a single large lipid droplet that compresses all other cellular components to one side. Beige adipocytes emerge under conditions such as cold ambient temperature when some white fat depots take on thermogenic functions and anatomical characteristics intermediate between brown and white adipocytes. Modified from (Contreras et al., 2016).

1.4 Brown Adipose Tissue and its role in hibernation

In the early stages of arousal from torpor, much of the increase in metabolic rate and T_b can be attributed to activation of BAT (Nizielski et al., 1989). BAT contains more, smaller, lipid droplets and a higher concentration of mitochondria compared to WAT (Figure 1.3). BAT mitochondria express very little ATP synthase, but do express a membrane protein called uncoupling protein-1 (UCP1). UCP1 belongs to a family of proteins which includes UCP3. In eutherian mammals UCP1 is expressed predominately, if not exclusively, in BAT (Laursen et al., 2015), whereas UCP3 is expressed predominately in muscle (Raimbault et al., 2001). When UCP1 is activated in BAT by adrenergic signalling, UCP1 uncouples the oxidation of metabolic substrates from ADP phosphorylation within the mitochondrial electron transport system (ETS). Some of the free energy released from substrate oxidation is used to pump protons across the inner mitochondrial membrane at ETS complexes I, III and IV. The rest of the free energy is released as heat. In most mitochondria this proton gradient powers ATP synthesis by ETS complex V (ATP synthase) when ADP is present within the mitochondrial matrix. In BAT, UCP1 activation dissipates the proton gradient without synthesizing ATP by allowing electrons to bypass complex V and flow through UCP1, thereby stimulating ETS substrate oxidation and proton pumping. As a result of this "futile cycle" of protons, all of the free energy released by ETS substrate oxidation is in the form of heat. This heat can be quickly dispersed to other parts of the body through the high vascularization of BAT.

In Arctic ground squirrels BAT gene expression patterns change markedly between spring/summer and hibernation (Yan et al., 2006). In 13-lined ground squirrels, expression of several BAT-specific genes, including those involved in mitochondrial metabolism and adrenergic signaling, increase from spring to autumn, before hibernation and without cold exposure (Hampton et al., 2013). This differential gene expression may contribute to an apparent peak in BAT cell proliferation in autumn (Hindle and Martin, 2014). By contrast BAT depots in warm-housed non-hibernators are minimal and require extensive acclimation to decreased T_a (Nakamura and Morrison, 2007).

Circannual changes in BAT gene expression in hibernators may also be reflected in BAT mass. From June through September the mass of axillary BAT pads of Arctic ground squirrels increased even though animals were maintained at constant T_a (20°C) and photoperiod (16h L:8h D; Feist et al., 1985). A more recent study showed increases in the mass of axillary BAT pads in 13-lined ground squirrels between spring and fall even though the animals were maintained on a constant 12h L:12h D photoperiod (Ballinger et al., 2016), though T_a was reported only as "room temperature". These and similar studies have assessed axillary BAT depot size by dissecting individual pads from euthanized animals, but BAT is distributed in several locations throughout the thorax (Figure 1.4; Oelkrug et al., 2015) so it is not clear how one, albeit major, depot reflects BAT changes across the whole animal. Moreover, thorax BAT depots are not always distinct from one another, and it is difficult to completely dissect an entire, discrete pad. My previous work (MacCannell et al., 2017) used Magnetic Resonance Imaging (MRI) to confirm that growth of BAT in hibernators occurs prior to the hibernation season, even when animals are held at constant warm T_a (22°C), with a photoperiod that was changed weekly to reflect that of the animals' natal origin (Carman, MB). The greatest increase in relative thorax BAT volume was between June and October before cold exposure. This observation contrasts with a study in the same species that found little change in the relative mass of dissected interscapular BAT pads, a single discrete pad in the thorax (Hindle and Martin, 2014). The MRI technique is more sensitive because it allows for repeated measures to assess changes to tissue volume or lipid content than manually dissecting and weighing the tissue.

In my thesis, I used MRI to identify and quantify WAT and BAT depots. MRI allows for repeated measurements of the same animal because animals do not have to be sacrificed, thereby minimizing interindividual variability. The MRI pulse sequence ***I***terative ***De***composition of water and fat with ***E***cho ***A***symmetry and ***L***east-squares estimation (IDEAL) (Fuller et al., 2006, Reeder et al., 2005), can separate the water and fat hydrogen signals of the entire animal. This technique allows for non-invasive identification of the location and proton density fat fraction (PDFF) (Equation 1) of each tissue throughout the entire volume of the animal. The PDFF value can be used to distinguish BAT and WAT from other tissues (Hines et al., 2010, Reeder et al., 2009).

BAT contains proportionately less lipid (30-70%) (Hu et al., 2010, Prakash et al., 2016, Rasmussen et al., 2013) than WAT (80-100%) and therefore a lower PDFF, allowing for differentiation between BAT and WAT and quantification of the volume of each.

$$\text{Fat fraction} = \frac{\text{Lipid } {}^{1}\text{H Signal}}{\text{Lipid } {}^{1}\text{H + Water } {}^{1}\text{H Signal}}$$

Equation 1: equation to calculate proton density fat fraction for IDEAL MRI

A fat depot located in the orbital cavity of hibernating 13-lined ground squirrels was discovered during the first IDEAL MRI study ever done on this species (MacCannell et al., 2017). This depot had a PDFF consistent with BAT (40.9±0.5%) (Figure 1.5) and was within the range of BAT verified by biopsy for other mammals (Hu et al., 2010, Prakash et al., 2016, Rasmussen et al., 2013). To my knowledge this fat depot has not been previously described. Thermal imaging of 13-lined ground squirrels induced to arouse (Appendix A) revealed a higher temperature around the ears and eyes, near the location of this orbital fat, than other parts of the head and the thorax. Thermal images of hibernating bears show increased temperature around the eyes (Laske et al., 2010). Also, torpid Arctic ground squirrels housed at -10°C showed a significantly higher temperature of the brain, BAT and neck compared to liver, rectum, WAT and gastrocnemius muscle (Barger et al., 2006). This observation in conjunction with the PDFF value resembling BAT, suggested that this tissue might be a BAT pad located in the head.

It was also brought to my attention that this fat depot could be the Harderian gland (Wei Li, personal communication). In mice, lipid comprises approximately 35% of the Harderian gland (Watanabe, 1980), which is within the bounds of the PDFF values used to identify BAT (i.e. 30–70%). However, the PDFF values measured near the ground squirrel heads ranged from 39–46%, higher than the reported lipid composition of mouse Harderian gland. Also, the reported 35% total lipid composition of Harderian gland is likely an upper limit of total lipid, as it was determined by chemical extraction (Watanabe, 1980), which would detect virtually all lipids. Water-fat MRI, on the other hand, only detects lipids that are 'mobile', especially TAGs, but not lipids found within membranes including most phospholipids and myelin, that would be extracted chemically

(Hines et al., 2010). I believe, therefore, that the MRI-detectable proton density fat fractions from this gland would be lower than that detected by chemical extraction. I was able to rule out this possibility with preliminary studies that the ground squirrel orbital fat contained no porphyrin, a characteristic of this gland (Payne, 1994). Subsequently I located and confirmed the 13-lined ground squirrel Harderian gland. This organ was located at the base of the optic nerve and was much smaller than the orbital fat depot. To my knowledge this was the first time this fat depot had been described.

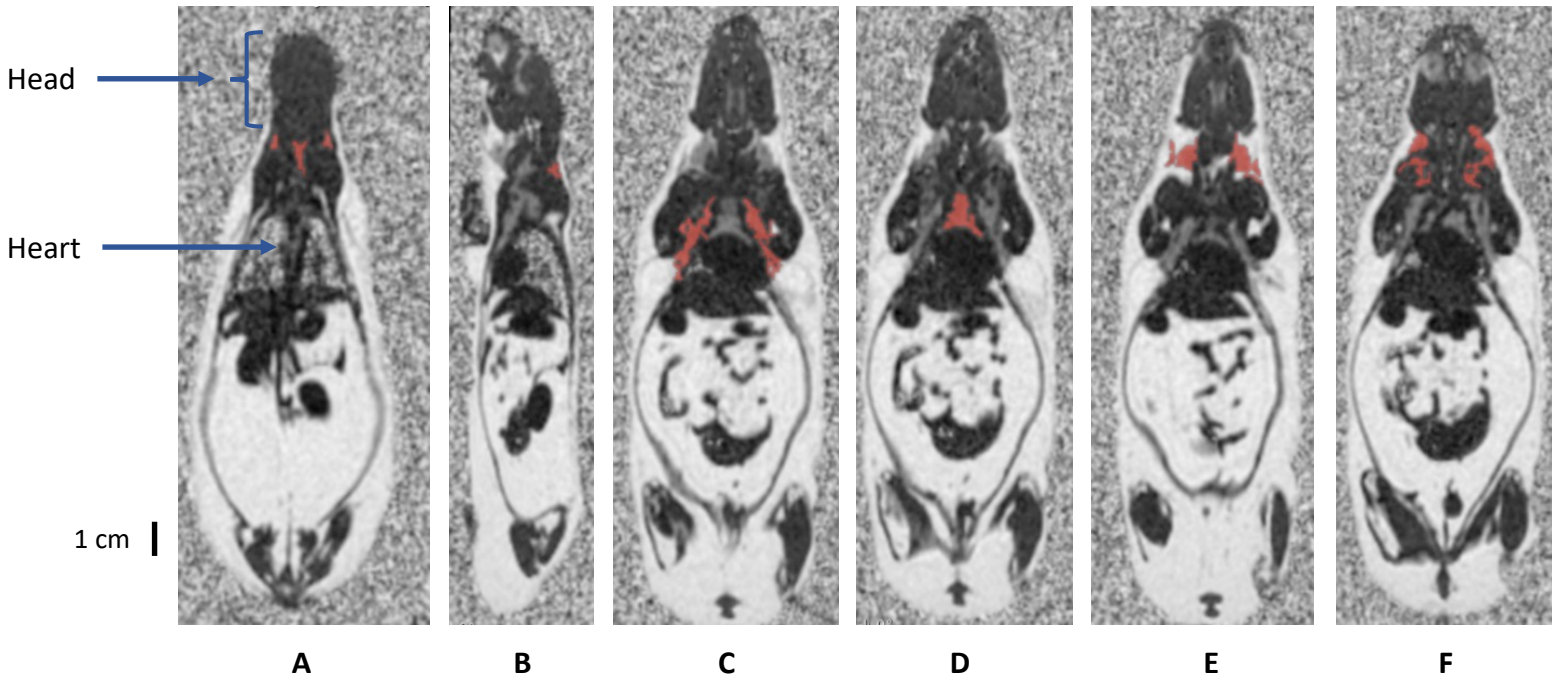

Figure 1.4 Water-fat Magnetic Resonance Imaging (MRI) reveals diffuse distribution of brown adipose tissue (BAT) within the ground squirrel thorax. Images were collected from the same animal on the same day (30 November 2015). The location of BAT (highlighted in red) broadly agrees with that pattern described in mice by Oelkrug et al. (2015), i.e. dorso-cervical (A, central depot), interscapular (B; lateral view with dorsal surface to right), axillary (C), intrathoracal (D), axillar/supraclavicular (E) and suprascapular (F). Modified from MacCannell et al. (2017).

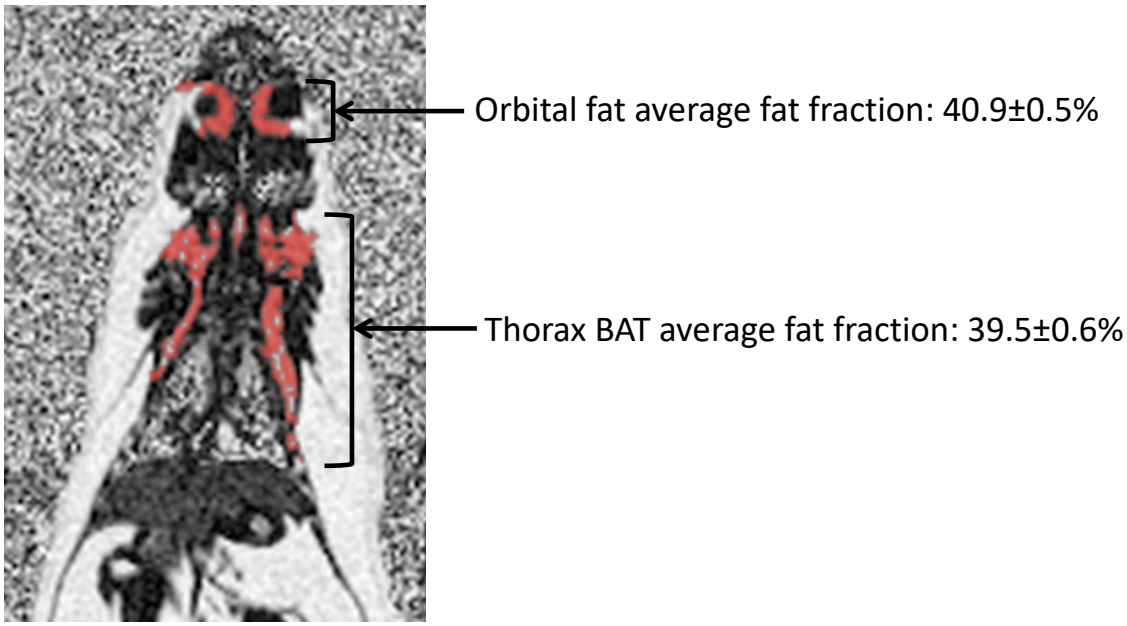

Figure 1.5 Proton density fat fraction (PDFF) magnetic resonance imaging (MRI) of a ground squirrel with the orbital fat and thorax brown adipose tissue (BAT) highlighted. Sample MRI slice of an animal housed in hibernating conditions (22°C from March – October and 5°C from October – March), MRI was taken form 30 November 2016. Areas highlighted in red indicate location of PDFF between 30-70%, expected values for BAT. Modified from MacCannell et al. (2017).

1.5 Objectives and Hypothesis

The 13-lined ground squirrel is a presumed obligate hibernator (Drew et al., 2007, Russell et al., 2010) but, to my knowledge no studies have confirmed the hibernation type as either facultative or obligate. Thus, I hypothesized that the 13-lined ground squirrel will hibernate regardless of environmental temperature and will show a circannual endogenous rhythm of body mass, WAT and BAT volume. I also investigated changes in WAT and BAT PDFF, and whether any patterns differed between subcutaneous and visceral WAT. In order to achieve this objective, I used water-fat MRI from animals housed at constant photoperiod and either cold (5°C) or warm (thermoneutral; 25°C) T_a to determine volume and lipid content. I predicted that body mass, WAT volume and BAT volume would increase in anticipation of hibernation, decrease during hibernation and recover after hibernation and that environmental temperature will not affect these changes.

An ancillary hypothesis was that the orbital fat depot is indeed BAT. I predicted therefore that it would contain UCP1 and have a histology similar to that of thorax BAT.

Chapter 2

2 Materials and methods

2.1 Experimental Animals

All procedures were approved by the University of Western Ontario Animal Care Committee (protocol 2012-016; Appendix B) and followed Canadian Council on Animal Care guidelines. A single wild-caught ground squirrel from Carman, MB gave birth to eight males in captivity on 9 July 2016. Ground squirrels were housed in individual plastic shoebox-style cages (26.7×48.3×20.3cm high) with dried corn cob bedding, paper nesting material (Crinkl-l'Nest, The Andersons, Inc.), and a cardboard tube (Bio-tunnels, K3557, Bioserve) for enrichment. Rat chow (LabDiet 5P00), dry dog food (Iams), and water were provided *ad libitum*, with sunflower seeds and corn provided three times a week. Each animal was weighed during weekly cage cleaning and at the time of MRI.

2.2 Environmental temperature effects

Once the ground squirrels were weaned from their mother on 8 August 2016 the juvenile animals were housed at 12h L:12h D and 21°C. Animals were then randomly divided into the two experimental groups: cold-housed (5°C) and the warm-housed (thermoneutral) group (25°C), n=4 for each group. Cold-housed animals had their initial MRI on 19 August 2016 and were then transitioned to an ambient temperature of 5°C by a decreasing the temperature 1°C/day. Warm-housed animals had their initial MRI on 22 August 2016 and were immediately moved into a 25°C chamber. For both groups a 12h L:12h D photoperiod was maintained. Torpor bouts were confirmed by the sawdust technique (Pengelley and Fisher, 1961), sawdust is placed on the back of a torpid squirrel and animals were observed daily for the presence of the sawdust. This technique was used because instrumenting these animals with T_b telemeters would have interfered with MRI.

2.3 Magnetic Resonance Imaging

Squirrels had MRIs approximately every three weeks. Scheduling constraints of the MRI required the two treatment groups to be scanned on alternating weeks (Figure 2.1). For

each MRI, ground squirrels were anaesthetized using isoflurane (4.5% induction, 2l/min O_2, maintenance 1.0-3.0%, 1 l/min O_2) for approximately 35min. Animals were placed on their ventral surface and, throughout MRI rectal body temperature and ventilation rates were monitored (Model 1030 Small animal monitoring and gating system, SA Instruments, INC, Stony Brock, NY USA). Imaging was performed at 3 Tesla (MR750, GE, Waukesha, WI, USA) using a 32-element cardiac receiver array (Invivo, Gainesville, FL, USA). T_1-weighted gradient echo (repetition time/echo time [TR/TE]=5.1ms/2.4ms, flip angle=15°, number of averages=4, total MRI time ~7min) produced images of the whole animal, used to identify anatomical features. IDEAL water-fat images (Figure 2.2A; TR/ΔTE=9.4ms/0.856ms, 6 echoes, flip angle = 4°, number of averages=4; total scan time ~ thirteen min) were collected for each squirrel with $0.933 \times 0.933 mm^2$ in-plane spatial resolution and 0.9mm slice thickness (Yu et al., 2008). Fat fraction was measured from the PDFF images, which represents the proportion of ^1H signal from mobile lipid relative to the cumulative ^1H signal from both lipid and water (Fuller et al., 2006, Reeder et al., 2005).

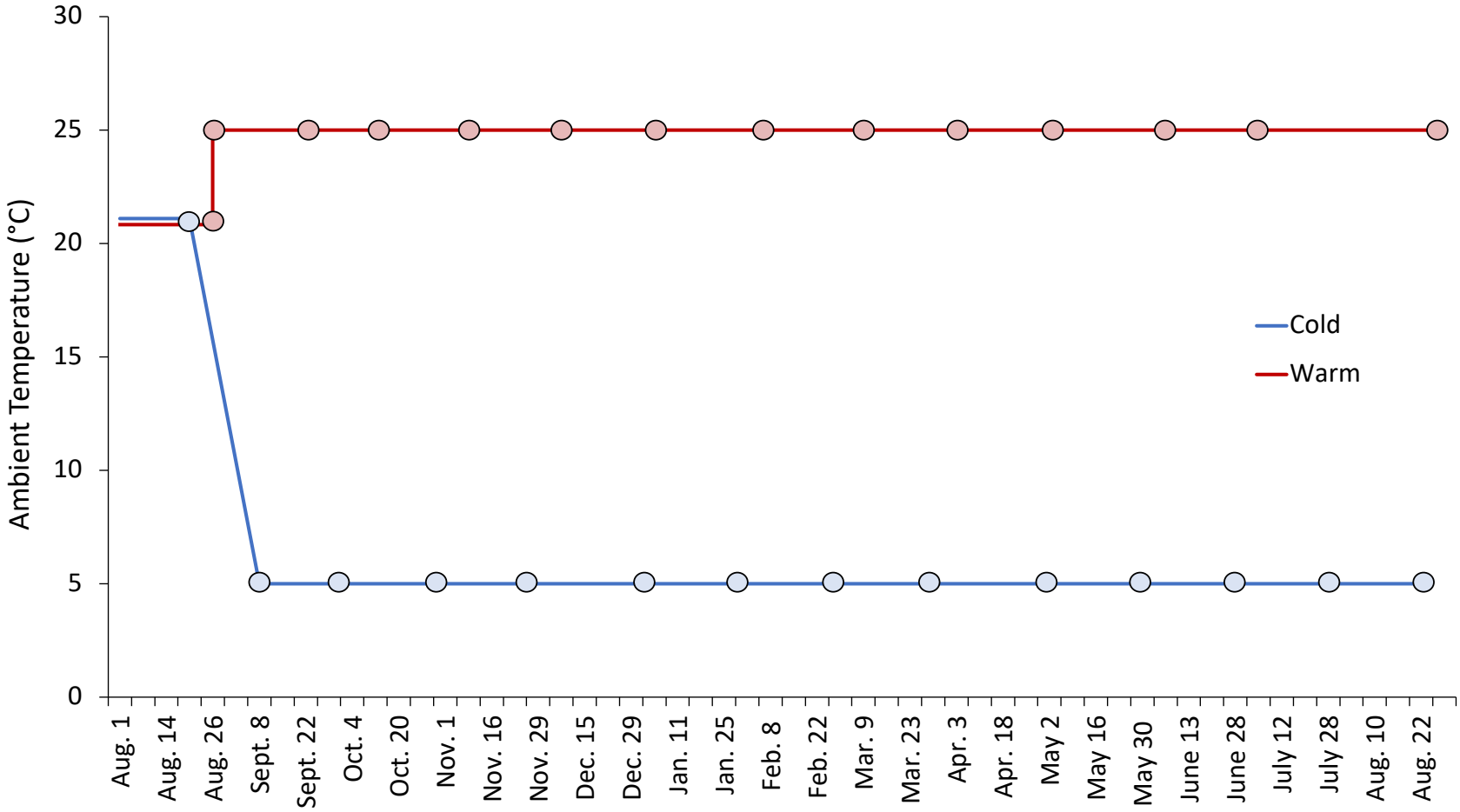

Figure 2.1 Timeline illustrating dates of magnetic resonance images (MRI) and ambient temperatures of animals. MRI began in August 2016 and was completed in August 2017. Blue line indicates ambient temperature of cold-housed (5°C) and red line indicates ambient temperature of warm-housed (25°C). The circles indicate date of MRI scan, data collected from the warm-housed animals on 4 August 2017 was lost. Immediately after the last MRI for each condition animals were sacrificed.

2.4 MRI Segmentation

The areas of interest from the MRI scans were selected by using the Osirix 5.6 (Bernex, Switzerland) 2D threshold region growing algorithm tool. This tool allows for specific PDFF parameters to be set, when an area of an MRI slice is selected, only the pixels with the set PDFF would be highlighted and included in the total area and PDFF calculations. BAT volumes were segmented using the segmentation parameters set to a lower threshold of 30 and an upper threshold of 70, (i.e. between 30% and 70% of the tissue volume consisted of lipid) based on segmentation guidelines adapted from earlier studies (Figure 2.2 B; Hu et al., 2010, Prakash et al., 2016, Rasmussen et al., 2013). WAT volumes were segmented with PDFF parameters set to a lower threshold of 80. The BAT of the warm group showed non-uniformity in the PDFF, so the BAT was segmented manually by drawing a region of interest around the entire BAT pad. T_1-weighted images were used to determine the location of the abdominal wall, which was used to separate visceral and subcutaneous WAT, which were measured separately (Figure 2.2 C and D). The segmentation was conducted on each MRI slice and the summed areas were multiplied by the slice thickness (0.9mm) to calculate total volume of the tissue. I assumed the density of tissue to be 0.9g/ml (Ross et al., 1991, Hoffmann et al., 1997) to calculate the mass of BAT and WAT, and divided this value by animals mass to calculate the percentage of total body mass represented by these tissues. To ensure accuracy all segmentation was conducted independently by two people, myself and a second reader (Prasiddha Parthasarathy), the results were compared between the two readers. This is a common practice in MRI studies (Espeland et al., 2013).

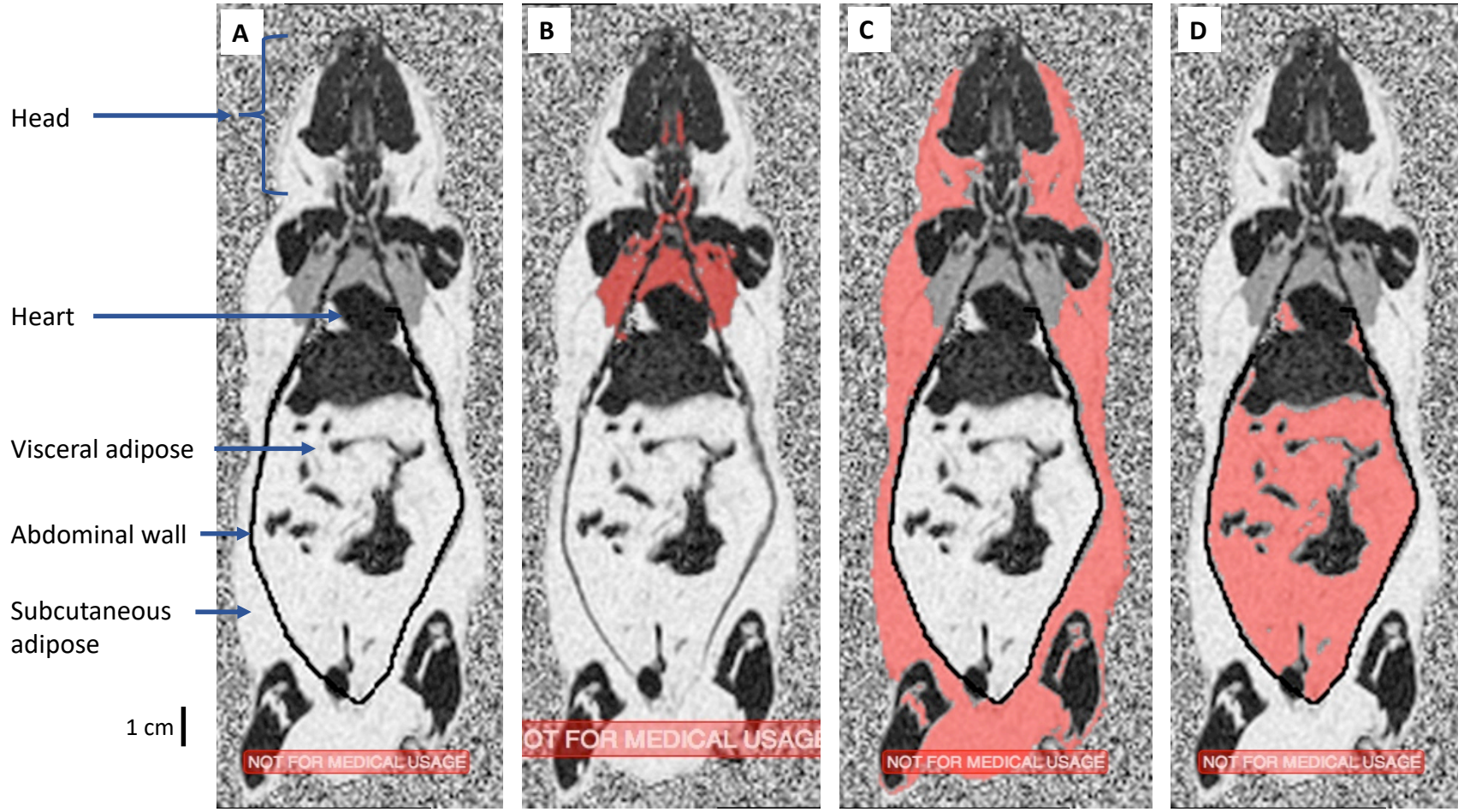

Figure 2.2 Sample magnetic resonance images (MRI) of a single 13-lined ground squirrel on 22 September 2016, with regions of interest indicated. Each image represents the same slice from the same animal. A sample water-fat image slice showing different tissues (A). Semi-automated segmentation determined area and proton density fat fraction of BAT (B), subcutaneous WAT (C) and visceral WAT (D).

2.5 Tissue Sampling

I collected tissues for immunoblot, citrate synthase and histological analyses. Following the final MRI in August 2017, animals were sacrificed with a 0.7ml intraperitoneal injection of Euthanyl (Bimeda-MTC Animal Health Inc., Cambridge, ON). Tissues were also collected from a hibernating animal which was housed at 22°C until October and then housed at 5°C until sacrificed in February. The eyelids and eye were removed to expose the optical cavity, the orbital fat pad located immediately behind the eye was removed, along with the Harderian gland located at the base of the optic nerve. The Harderian gland was isolated from a Long-Evans Rat and used as a control (Covelli, Vincenzo, 1972). The squirrel was decapitated, the skull was cut along the medial line to expose the brain, and the forebrain was removed from the skull. The BAT pads located adjacent to the rib cage were removed from the thorax. The heart was removed, and the right and left ventricle were retained. The gastrocnemius muscle and WAT from the right side of the abdomen of both subcutaneous and visceral adipose tissue were removed. All tissue samples removed were individually wrapped in aluminum foil and immediately immersed in liquid N_2. Tissues were stored at -80°C until analyzed. Tissue samples included in immunoblot analysis were all isolated from the 13-lined ground squirrel: orbital fat, Harderian gland, heart, BAT, forebrain, and gastrocnemius muscle. Tissues used in citrate synthase analysis included BAT from the warm-housed animals, BAT and WAT from a hibernating mammal. For histological analysis, squirrel WAT, BAT, orbital fat and rat Harderian gland tissues were removed immediately after sacrificing the animals and placed in 10% Formalin for 24 hours and then transferred to 70% ethanol until samples could be processed.

2.6 Immunoblot Analysis

Immunoblots were performed to quantify two different proteins: UCP1 to determine molecular changes of BAT from warm group animals (section 3.3), and UCP1 and UCP3 to determine if the orbital fat contained any uncoupling protein homologues (section 3.3). These samples were homogenized in Radioimmunoprecipitation assay buffer (RIPA; 50mM Tris, 150mM NaCl, 1% SDS, 0.5% sodium deoxycholate and 1% Triton X-100)

for total protein extraction. Samples were centrifuged at 4°C and 10,000*g* for 20min before being stored at -80°C. Total protein was determined with a detergent compatible protein assay (Lowry et al., 1951; BioRad 5000116) to ensure accurate loading. Upon completion of the reaction (15min), the absorbance (750nm) was measured using a spectrophotometer (SpectraMax 340PC, Molecular Devices, Toronto ON), and compared to standards consisting of bovine serum albumin (BSA) dissolved in RIPA.

For each tissue, 30µg of homogenate protein were separated by electrophoresis using 10% sodium dodecyl sulfate–polyacrylamide gels. Gels were run at 180V for 1h in a running buffer (25mM Tris, 190mM glycine, 0.1% SDS), then transferred to polyvinylidene fluoride membranes. Transfer of proteins from gel to membrane occurred at 4°C at 100V for 2h. After transfer, membranes were blocked with 5% BSA in Tris-buffered saline and Tween-20 (TBST; 20mM Tris, 143mM NaCl, 0.05% Tween-20) under steady agitation for 2h. Membranes were probed with UCP1 (primary-antibody 1:1000 (abcam ab10983)) or UCP3 (primary-antibody 1:1000 (abcam ab10985)) overnight at 4°C. Rabbit anti-goat secondary antibody (1:20000; abcam ab205718) was incubated for 1h at room temperature under steady agitation. The membrane was washed three times for 10min in Tris-buffered saline and Tween-20 (TBST). Bands were visualized using Luminata Forte ECL (Millipore) using a VersaDoc MP5000 imaging system (BioRad). Bands were quantified using the densitometry analysis tool in ImageLab 3.0 (BioRad) and standardized to total protein in each lane, determined via Amido Black staining to confirm accurate loading (Wilson, 1983).

2.7 Citrate Synthase Assay

I conducted citrate synthase assays to identify changes in mitochondrial content of BAT in animals housed in constant warm conditions. I used BAT and WAT of a single animal housed in hibernating conditions for comparison (22°C from March – October and 5°C from October – March, sampled in February). Citrate synthase (E.C. 2.3.3.1.) activity, is a validated biomarker for mitochondrial abundance (Boushel et al., 2007, Mogensen et al., 2006). Frozen tissues were powdered with motor and pestle before being homogenized in nine volumes of buffer (25mM HEPES, 0.1% Triton X-100, 2mM EDTA). Samples were centrifuged for five minutes at 4°C at 2000*g*, and the supernatant

was retained. I conducted all assays in 96-well polystyrene microplates at 37°C. Assays were conducted in triplicates, each well contained; 50mM Tris, pH 8.0, 0.15mM DTNB, 0.15mM acetyl coenzyme A. Plates were allowed to equilibrate to room temperature in the spectrophotometer for 5min before 3µL of homogenate was added to every well. Oxaloacetate (0.33mM) was added to experimental wells only. Plate absorbance was read at 412nm for 5min. Total protein from each tissue sample was quantified using a detergent-compatible protein assay (Lowry et al., 1951), described in section 2.4.

2.8 Statistical Analyses

All values are presented as mean±S.E.M. All statistical analysis for BAT and WAT depot volumes and PDFF was performed using SPSS (IBM Corp. Released 2013. IBM SPSS Statistics for Windows, Version 22.0. Armonk, NY: IBM Corp.) using repeated measures ANOVA and Greenhouse geisser correction. Pearson's correlation was used to examine any relationship between the PDFF of BAT and both UCP1 content and citrate synthase activity.

2.9 Histology

I performed hematoxylin and eosin (H&E) histology on BAT, orbital fat and WAT from 13-lined ground squirrels, as well as the Harderian gland from a Long-Evans rat. The small size of the 13-lined ground squirrel Harderian gland made it impractical to obtain histological images of comparable quality to the rat. Tissues were processed and embedded in paraffin wax blocks with a Leica ASP300 fully enclosed paraffin wax tissue processor. Tissues (n=2) were processed and stained at the UWO Robarts Molecular Pathology Core Facility. I imaged the slides at the Biotron Integrated Microscopy, Western University using a Zeiss Axioimager Z1 Upright Fluorescent/Compound microscope.

Chapter 3

3 Results

3.1 Total body mass of animals

Before weaning, all of the juveniles increased in mass at the same rate, with no significant difference between the groups before animals were separated into the two temperature treatments. The cold group began entering torpor on 28 September 2016 and maintained consistent torpor (with periodic arousals) until 18 March 2017, with the last animal permanently arousing on 3 April 2017. I observed that animals in the warm group were active, and eating, throughout the winter and there was no indication that they ever entered torpor, indicating that these animals might not be obligate hibernators. Both cold and warm groups increased body mass until mid-September (Figure 3.1). The warm group maintained a mean body mass of 266.9±1.8g until April. The body mass of the cold group declined steadily through mid-March, falling 29.1% from 233.5±8.8g to 165.5±13.2g. After torpor bouts stopped in April 2017, the cold-housed steadily gained mass through the end of April, between April and August 2017, the warm group increased their body mass steadily, but the cold group did not (Figure 3.1). There is a significant interaction between time and temperature on body mass ($F_{(3.1, 18.8)}$=15.0, $P<0.001$).

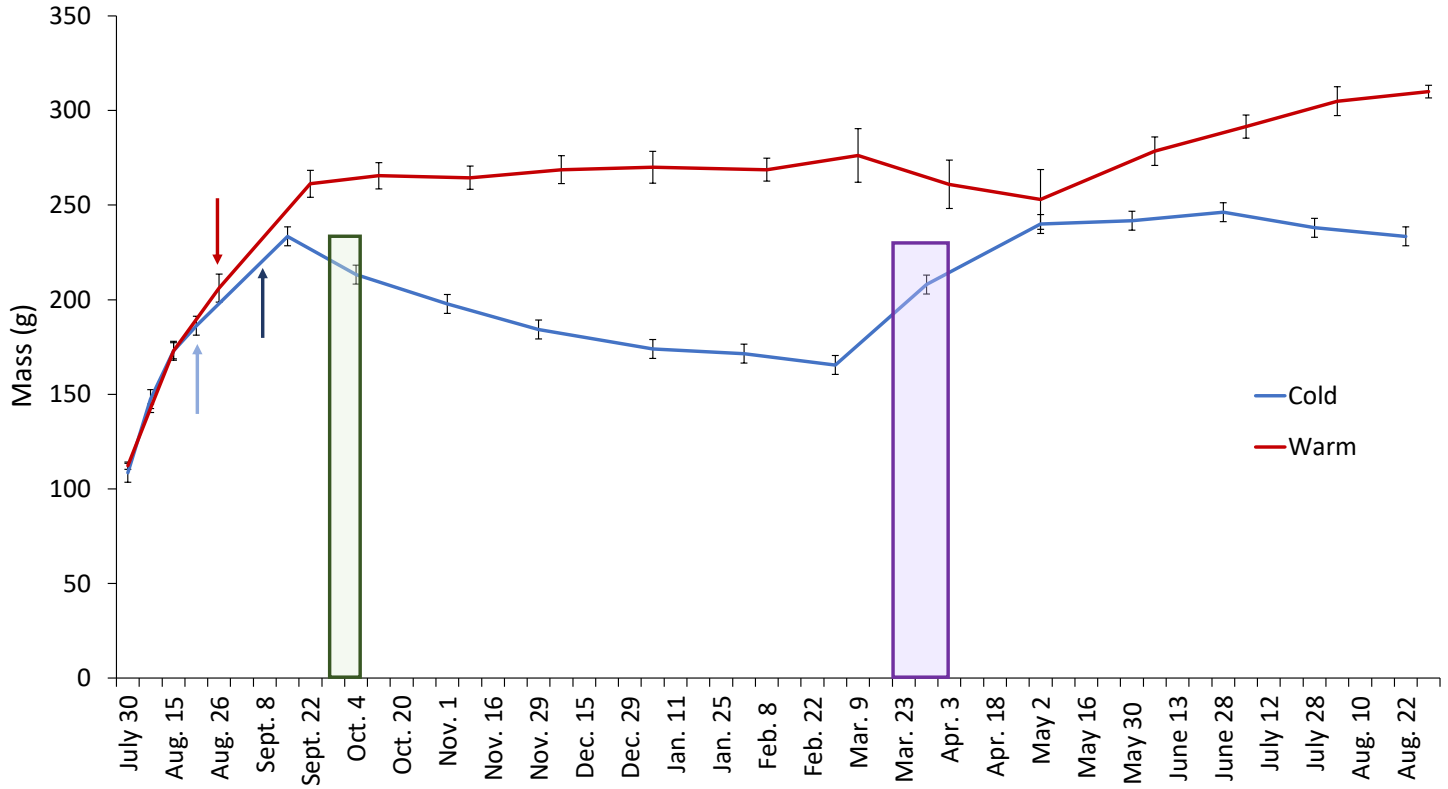

Figure 3.1 Thirteen-lined ground squirrel body mass over an entire year. The red line represents animals housed at 25°C and the blue line represents animals housed at 5°C, both groups had a 12h L:12h D photoperiod. Data are presented as mean±SEM, *n*=4 for each group. The green box indicates the range of initial torpor bouts for cold-housed animals (beginning 28 September 2016). The purple box indicates the range of terminal arousals (18 March - 3 April 2017). Light blue arrow indicates the initial scan for cold and the day temperature was dropped 1°C /day (19 August 2016). Dark blue arrow indicates the day the ambient temperature of the cold group reached 5°C (6 September 2016). The red arrow indicates the initial MRI scan for warm animals and the day they were transferred to 25°C (26 August 2016). There is a significant effect of time ($F_{(3.1, 18.8)}$=76.2, P<0.001), temperature ($F_{(1, 6)}$=27.8, P=0.002), and interaction between time and temperature ($F_{(3.1, 18.8)}$=15.0, P<0.001) on mass.

3.2 Environmental temperature effects on white adipose tissue

All measurements used in this study were confirmed by a second reader with a confidence of 99.2% between the two readers. Changes in WAT volume did not follow the same pattern as body mass. There is a significant effect of temperature ($F_{(1, 6)}$=12.6, P=0.012) on the percentage of body mass comprised of WAT (assuming a density of 0.9g/ml), the warm-housed group was consistently higher than the cold-housed group after the first scan in August 2016 (Figure 3.2). The warm group maintained consistent relative WAT content, of approximately 53.9±0.7% body mass, from 22 September to 8 February. Between February and March, however, this value fell to the lowest point of 34.4±3.1%. The cold group showed a steady decline from 42.6±0.9% in September to 18.7±2.1% in March. Between March and August, the warm group significantly increased their WAT content to the same values as early winter, 55.5±2.7%, whereas in the cold-housed group WAT remains quite steady at 21.8±0.6%. The pattern seen in the % body mass comprised of BAT is also reflected in the absolute volume of WAT (Figure 2B). There is no significant interaction between time and temperature in both the mass corrected WAT ($F_{(3.1, 18.4)}$=6.1, P=0.004) and absolute volume of WAT ($F_{(2.3, 13.8)}$=7.7, P=0.005).

In addition to quantifying total WAT, I also analyzed visceral and subcutaneous WAT separately. This analysis showed that the patterns for both depots generally follow that of total WAT, with subcutaneous WAT comprising the majority (approximately 65%) of total WAT, in both warm and cold groups (Figure 3.3). However, the PDFF of the visceral WAT in warm-housed animals was 3.1±0.1% higher than subcutaneous values throughout the year (Figure 3.4A). For cold-housed animals, the visceral WAT PDFF was also 2.8±0.1% higher than the subcutaneous WAT for most of the year. (Figure 3.4B). There is a significant effect of time ($F_{(2.0, 12.1)}$=9.4, P=0.003) and temperature ($F_{(1, 6)}$=67.3, P<0.000), but no significant interaction between time and temperature ($F_{(2.0, 12.1)}$=0.7, P=0.504) for both the visceral and subcutaneous WAT in the cold and warm group.

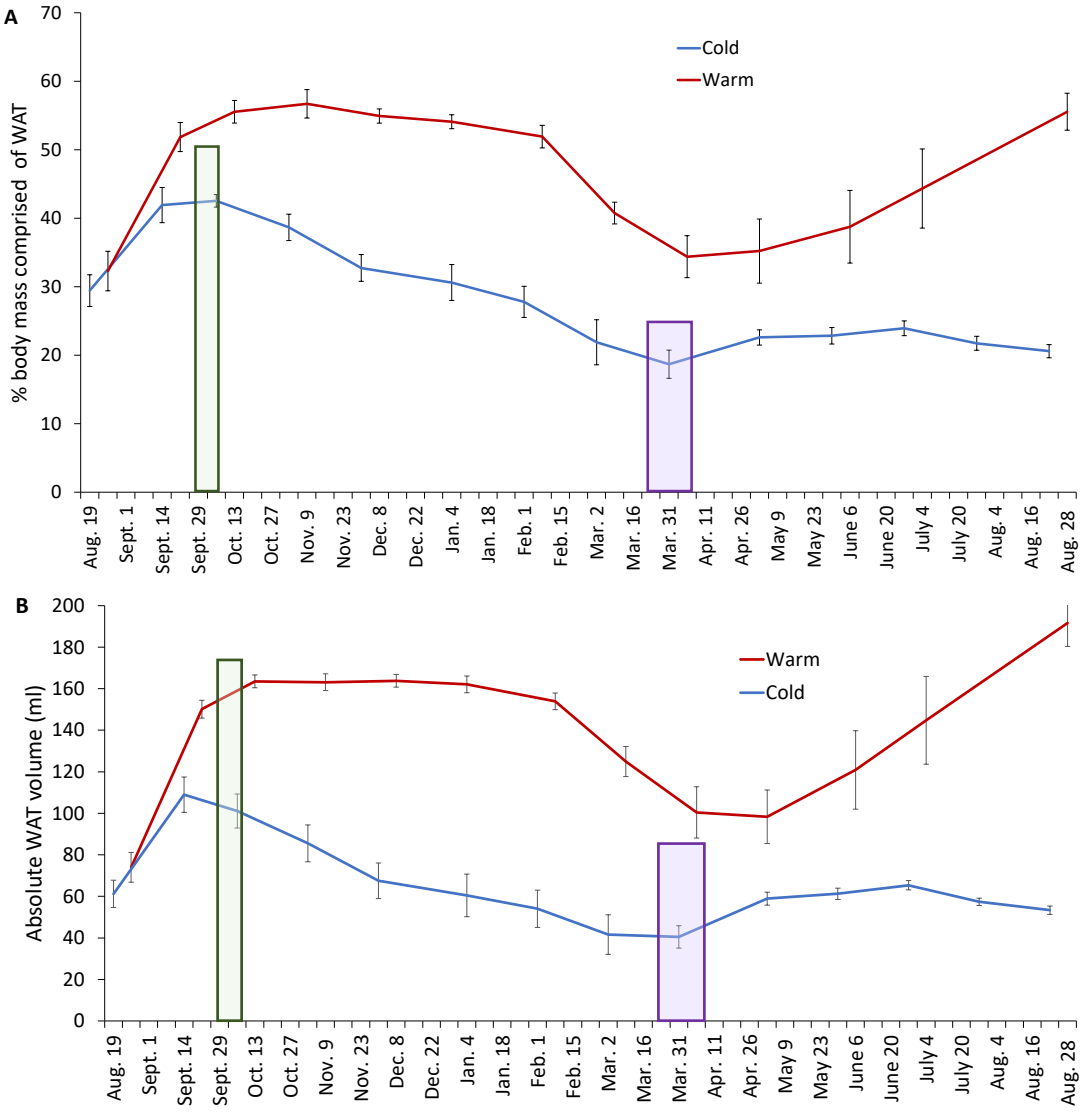

Figure 3.2 Percentage of body mass comprised of white adipose tissue (WAT) (assuming 0.9g/ml) (A) and absolute volume of WAT (ml) (B). The red line represents animals housed at 25°C and the blue line represents animals housed at 5°C, both groups had a 12h L:12h D photoperiod. Data are presented as mean±SEM, *n*= 4 for each group. The green box indicates the range of initial torpor bouts for cold-housed animals (beginning 28 September 2016). The purple box indicates the range of terminal arousals (18 March - 3 April 2017). There is a significant effect of time ($F_{(3.1, 18.4)}$=24.9, P<0.000), temperature ($F_{(1, 6)}$=12.6, P=0.012) and interaction between time and temperature ($F_{(3.1, 18.4)}$=6.1, P=0.004) on the percent of body mass comprised of WAT. There is also a significant effect of time ($F_{(2.3, 13.8)}$=14.0, P<0.001), temperature ($F_{(1, 6)}$=98.1, P<0.001), and interaction between time and temperature ($F_{(2.3, 13.8)}$=7.7, P=0.005) on the absolute volume of WAT.

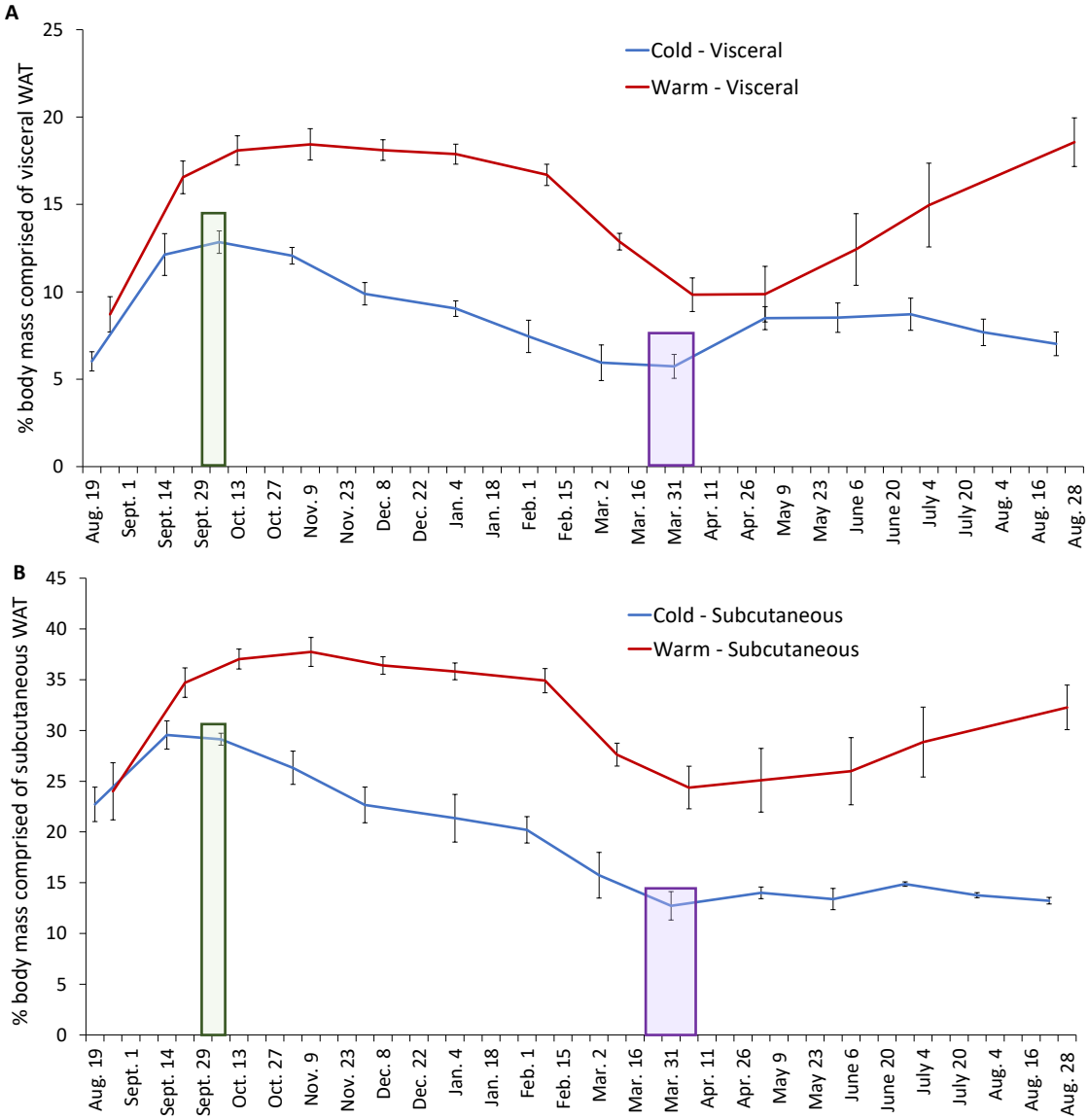

Figure 3.3 Quantity of visceral (A) and subcutaneous (B) white adipose tissue (WAT) relative to body mass (assuming 0.9g/ml). The red line represents animals housed at 25°C and the blue line represents animals housed at 5°C, both groups had a 12h L:12h D photoperiod. Data are presented as mean±SEM, *n*=4 for each group. The green box indicates the range of initial torpor bouts for cold-housed animals (beginning 28 September 2016). The purple box indicates the range of terminal arousals (18 March - 3 April 2017). There is a significant effect of time ($F_{(3.2, 19.0)}$=18.7, P<0.001), temperature ($F_{(1, 6)}$=47.8, P=0.001), and interaction between time and temperature ($F_{(3.2, 19.0)}$=5.5, P=0.006) on the percent of body mass comprised of visceral adipose tissue. There is also a significant effect of time ($F_{(2.9, 17.3)}$=34.7, P<0.001), temperature ($F_{(1, 6)}$=36.2, P=0.001), and interaction between time and temperature ($F_{(2.9, 17.3)}$=6.8, P=0.003) on the percent of body mass comprised of subcutaneous adipose tissue.

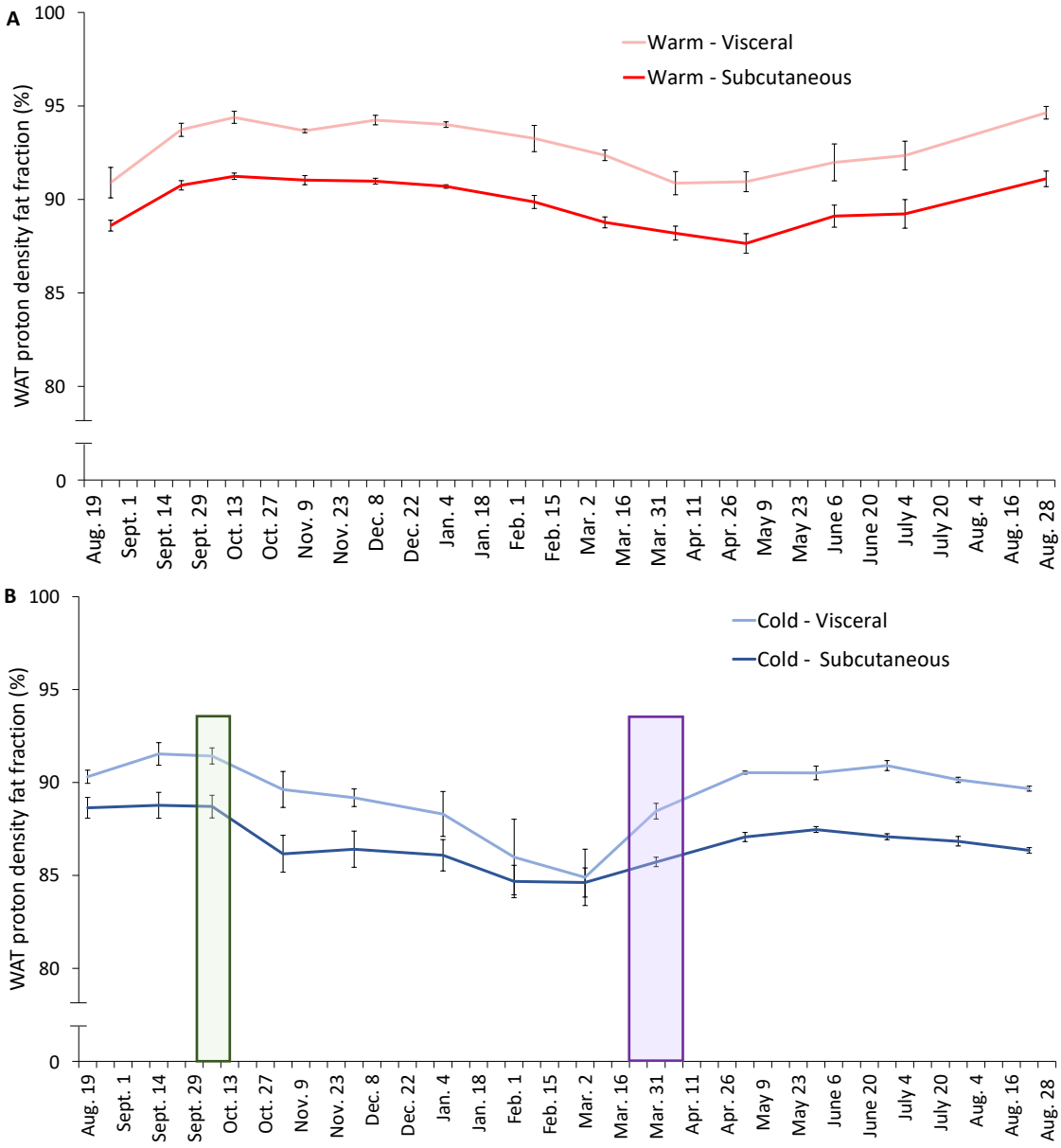

Figure 3.4 Proton density fat fraction (PDFF) values of visceral and subcutaneous white adipose tissue (WAT) in warm-housed (A) and cold-housed (B) animals. The lighter colored lines are visceral adipose, and the darker lines are subcutaneous adipose. Data are presented as mean±SEM, *n*=4 for each group. The green box indicates the range of initial torpor bouts for cold-housed animals (beginning 28 September 2016). The purple box indicates the range of terminal arousals (18 March - 3 April 2017). There is a significant effect of time ($F_{(2.0, 12.1)}$=9.4, P=0.003) and temperature ($F_{(1, 6)}$=67.3, P<0.001), but no significant interaction between time and temperature ($F_{(2.0, 12.1)}$=0.7, P=0.504) of visceral and subcutaneous WAT in warm-housed animals. There is also a significant effect of time ($F_{(2.5, 15.3)}$=11.5, P<0.001) and temperature ($F_{(1, 6)}$=23.3, P=0.003), but no significant interaction between time and temperature ($F_{(2.5, 15.3)}$=1.1, P=0.380) of visceral and subcutaneous WAT in cold-housed animals.

3.3 Environmental Temperature effects on brown adipose tissue

Between August and October, the relative content of BAT increased at least two-fold in both cold and warm groups (Figure 3.5A). Subsequently BAT content remained fairly constant in both groups until February, with the cold group's BAT comprising 2.0±0.0% of body mass and the warm group 1.7±0.8% of body mass. Between February and August BAT content decreased from 2.0±0.1% to 1.1±0.0% in the cold group, but in the warm group BAT fell as low as 0.5±0.0%. The absolute volume of BAT followed a similar pattern to that of the percent body mass comprised of BAT values, except the cold-housed animals had less BAT volume in the winter, between November and February, than the warm-housed animals (Figure 3.5B). There is no significant effect of temperature on the absolute volume of BAT ($F_{(1, 6)}$=0.3, P=0.599), but there is on the percent body mass comprised of BAT ($F_{(1, 6)}$=12.6, P=0.012), there is a correlation between body mass and BAT volume.

The PDFF of thoracic BAT ranged from 35.6–54.6%, typical of BAT from small mammals (Rasmussen et al., 2013). The PDFF of BAT in warm-housed animals remained constant, at 47.4±0.6%, throughout the year (Figure 3.5C). There is no significant effect of time ($F_{(2.4, 7.3)}$=2.7, P=0.127), temperature ($F_{(1, 6)}$=1.0, P=0.382) or interaction between time and temperature ($F_{(2.4, 7.3)}$=2.4, P=0.155) on the PDFF of BAT.

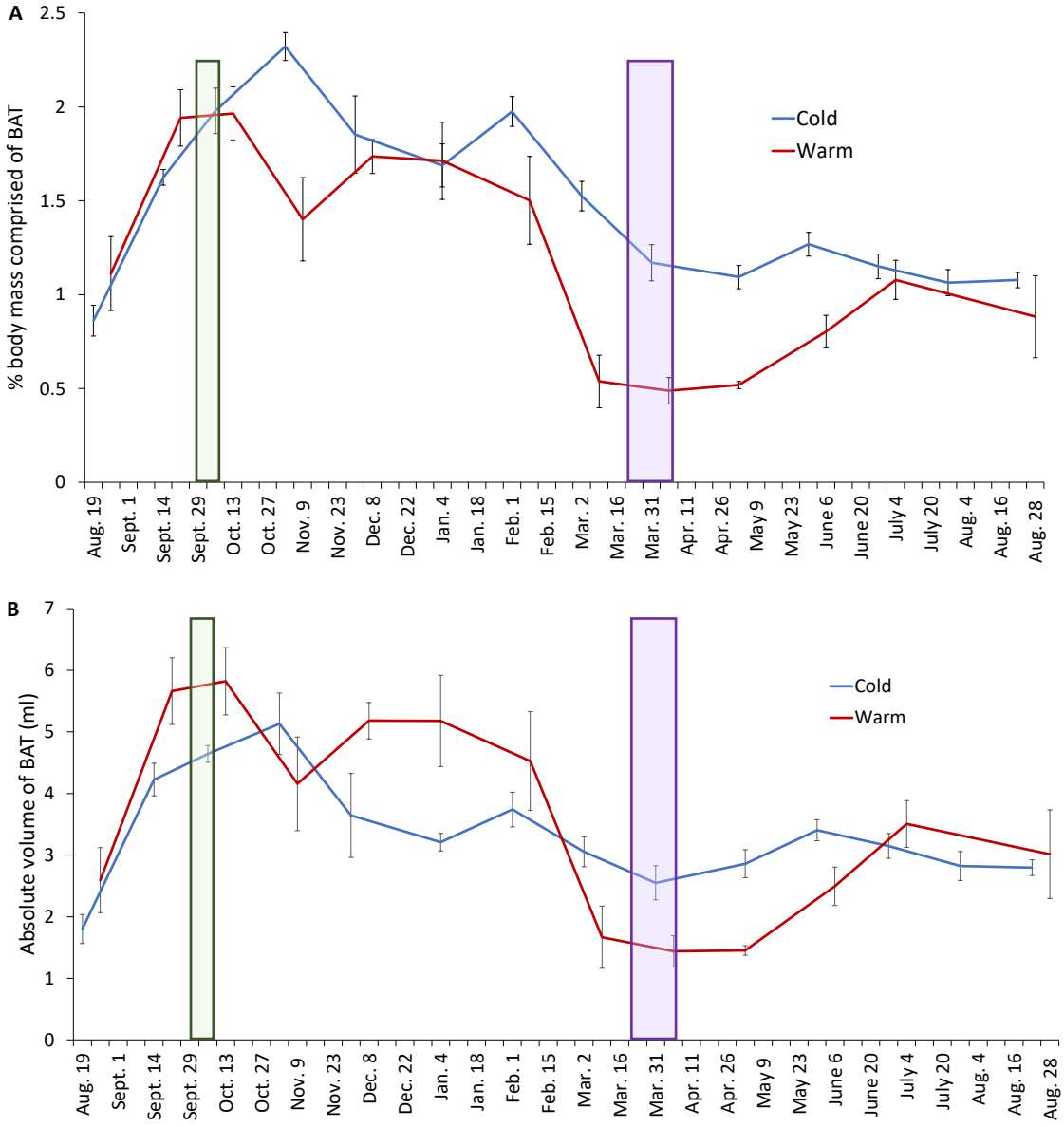
A
% body mass comprised of BAT
2.5
2
1.5
1
0.5
0
Cold
Warm
Aug. 19
Sept. 1
Sept. 14
Sept. 29
Oct. 13
Oct. 27
Nov. 9
Nov. 23
Dec. 8
Dec. 22
Jan. 4
Jan. 18
Feb. 1
Feb. 15
Mar. 2
Mar. 16
Mar. 31
Apr. 11
Apr. 26
May 9
May 23
June 6
June 20
July 4
July 20
Aug. 4
Aug. 16
Aug. 28
B
Absolute volume of BAT (ml)
7
6
5
4
3
2
1
0
Cold
Warm
Aug. 19
Sept. 1
Sept. 14
Sept. 29
Oct. 13
Oct. 27
Nov. 9
Nov. 23
Dec. 8
Dec. 22
Jan. 4
Jan. 18
Feb. 1
Feb. 15
Mar. 2
Mar. 16
Mar. 31
Apr. 11
Apr. 26
May 9
May 23
June 6
June 20
July 4
July 20
Aug. 4
Aug. 16
Aug. 28

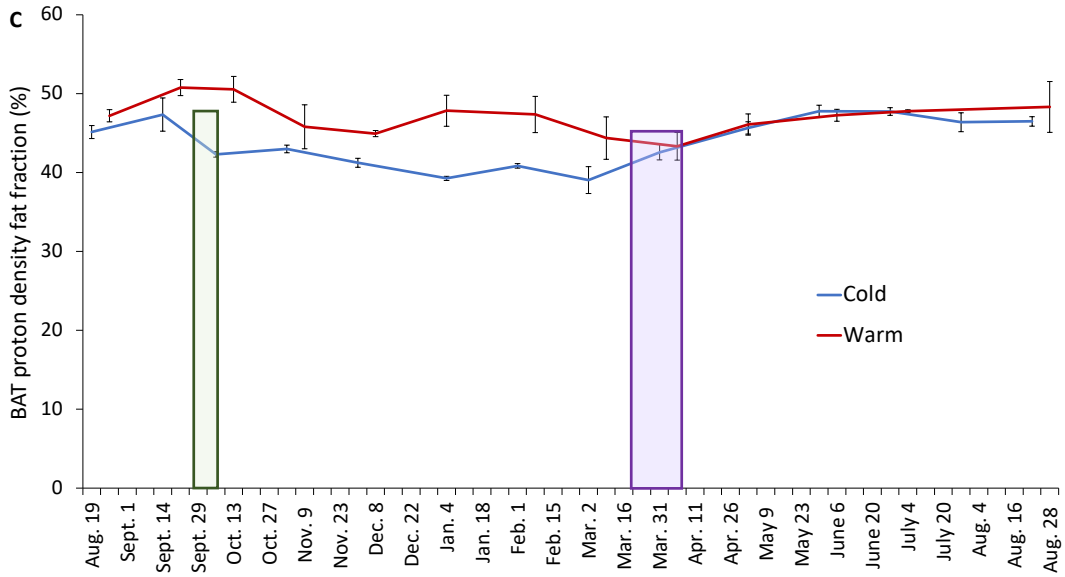

Figure 3.5 Percentage of body mass comprised of brown adipose tissue (BAT) (assuming 0.9g/ml) throughout one year (A), absolute volume of BAT (ml) (B) and corresponding proton density fat fraction (PDFF) (C). The red line represents animals housed at 25°C and the blue line represents animals housed at 5°C, both groups had a 12h L:12h D photoperiod. Data are presented as mean±SEM, *n*=4 for each group. The green box indicates the range of initial torpor bouts for cold-housed animals (beginning 28 September 2016). The purple box indicates the range of terminal arousals (18 March - 3 April 2017). There is a significant effect of time ($F_{(3.1, 18.4)}$=24.9, P<0.001), temperature ($F_{(1, 6)}$=12.6, P=0.012) and interaction between time and temperature ($F_{(3.1, 18.4)}$=6.1, P=0.004) of percent body mass comprised of BAT. There is also a significant effect of time ($F_{(2.6, 15.6)}$=18.1, P<0.001), but not temperature ($F_{(1, 6)}$=0.3, P=0.599), and a significant interaction between time and temperature ($F_{(2.6, 15.6)}$=13.5, P=0.016) of the absolute volume of BAT. There is no significant effect of time ($F_{(2.4, 7.3)}$=2.7, P=0.127), temperature ($F_{(1, 6)}$=1.0, P=0.382) and interaction between time and temperature ($F_{(2.4, 7.3)}$=2.4, P=0.155) on the PDFF of BAT.

IDEAL images of BAT showed temperature effects of BAT composition in warm-housed animals. One of the four warm animals showed uniform PDFF throughout the thorax BAT depot over the entire year, resulting in PDFF values similar to animals that hibernated in the cold (MacCannell et al., 2017). The IDEAL images from the other two warm-housed animals showed thorax BAT in the spring that did not appear uniform in terms of PDFF (Figure 3.6). The last animal had variable PDFF throughout the year, and therefore was omitted of the analysis. Manual segmentation revealed regions within the BAT with PDFF values above 70%, more typical of WAT, and therefore not detected by the semi-automated segmentation algorithm.

A higher PDFF value correlated with higher UCP1 expression relative to total protein for thorax BAT in warm-housed animals and a hibernating comparison (Figure 3.7) ($r=-0.986$, $P<0.001$). Citrate synthase activity from the same animals showed a similar pattern, with increased citrate synthase activity correlating with increase PDFF values (Figure 3.8) ($r=-0.946$, $P<0.005$). The citrate synthase activity from BAT in warm-housed animals with non-uniform BAT was comparable to levels in WAT from a hibernating animal.

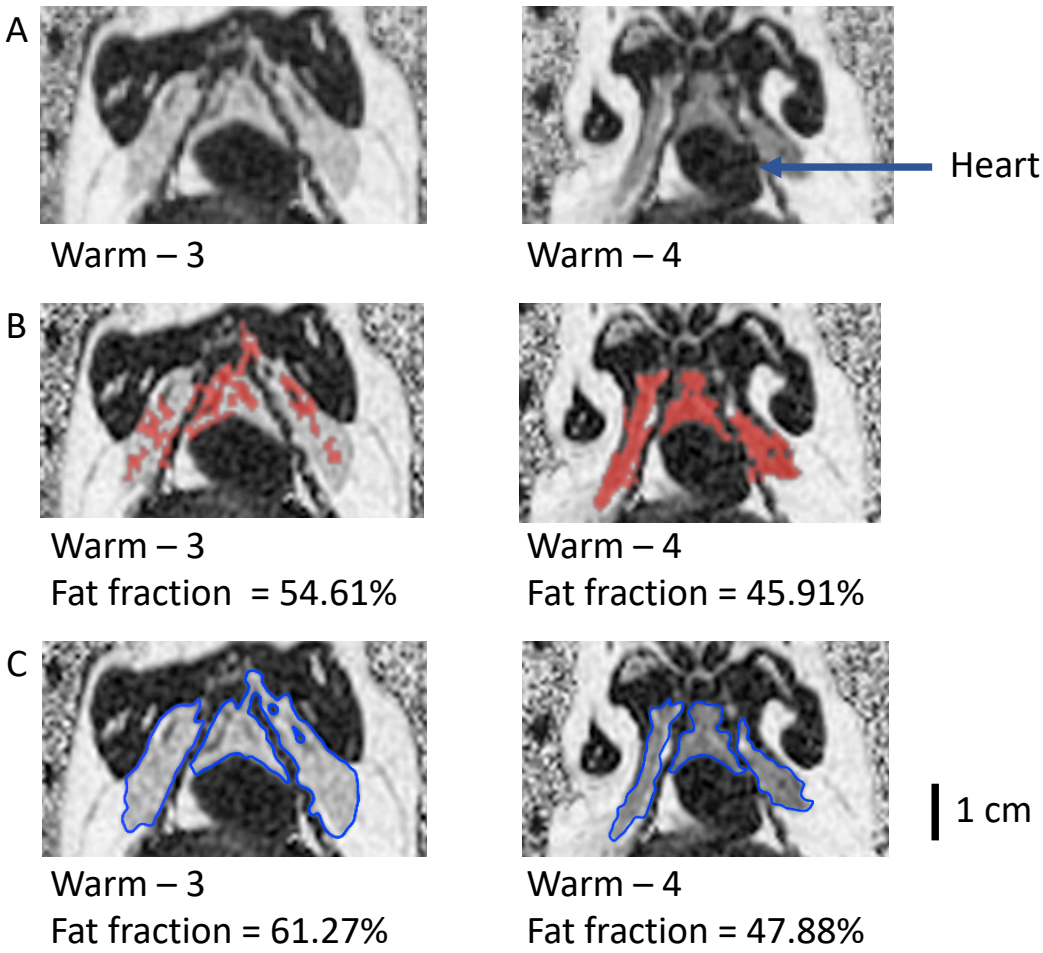

Figure 3.6 Magnetic Resonance Imaging (MRI) proton density fat fraction (PDFF) images showing a coronal slice of the chest of two warm-housed animals. Images were initially segmented using the semi-automated threshold region growing tool, PDFF corresponding to BAT (30-70% PDFF); these regions are highlighted in red (B). Animal Warm-4 showed uniform PDFF values throughout the BAT volume. Warm-3 showed non-uniform BAT with PDFF values >70% (gray regions within depot). Manual segmentation of the entire BAT volume was used to determine total PDFF of the depot (C). In animal Warm-4 manual segmentation did not alter the PDFF greatly, but in animal Warm-3 this process yielded a much higher value.

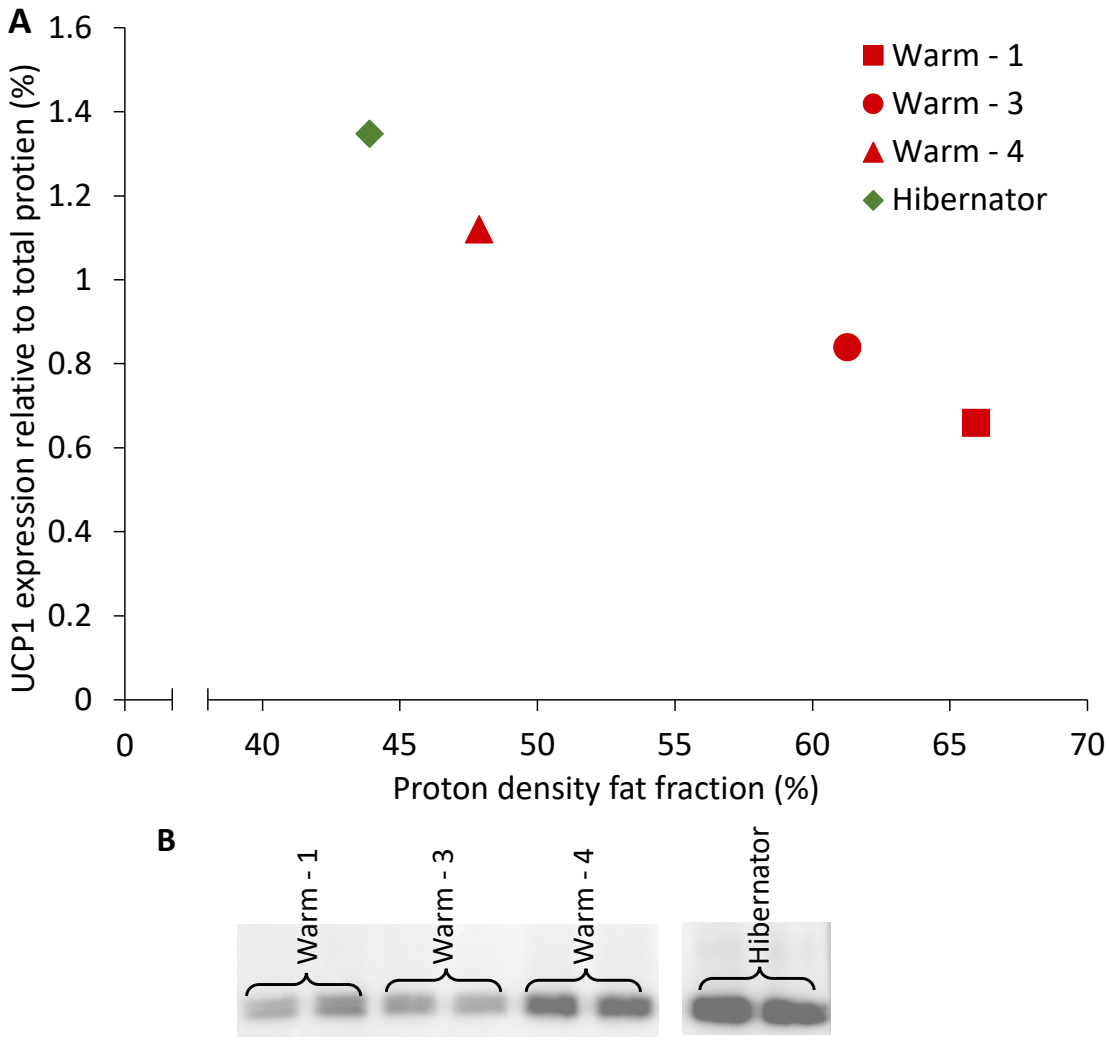

Figure 3.7 A) Relationship between uncoupling protein 1 (UCP1) protein content and mean brown adipose tissue (BAT) proton density fat fraction (PDFF) in warm-housed animals with non-uniform BAT (warm – 1 and warm – 3), uniform BAT (warm – 4) and a hibernating animal (animal housed at 22°C until October and then housed at 5°C until sacrificed in February) related to their respective PDFF values, r=-0.986, P<0.001. B) Samples of immunoblots used to calculate UCP1 content (Fig. 3.7A). Immunoblots were performed as technical replicates, with band intensity expressed relative to total protein quantity. Animals with non-uniform BAT show decreased UCP1 quantity compared to uniform BAT.

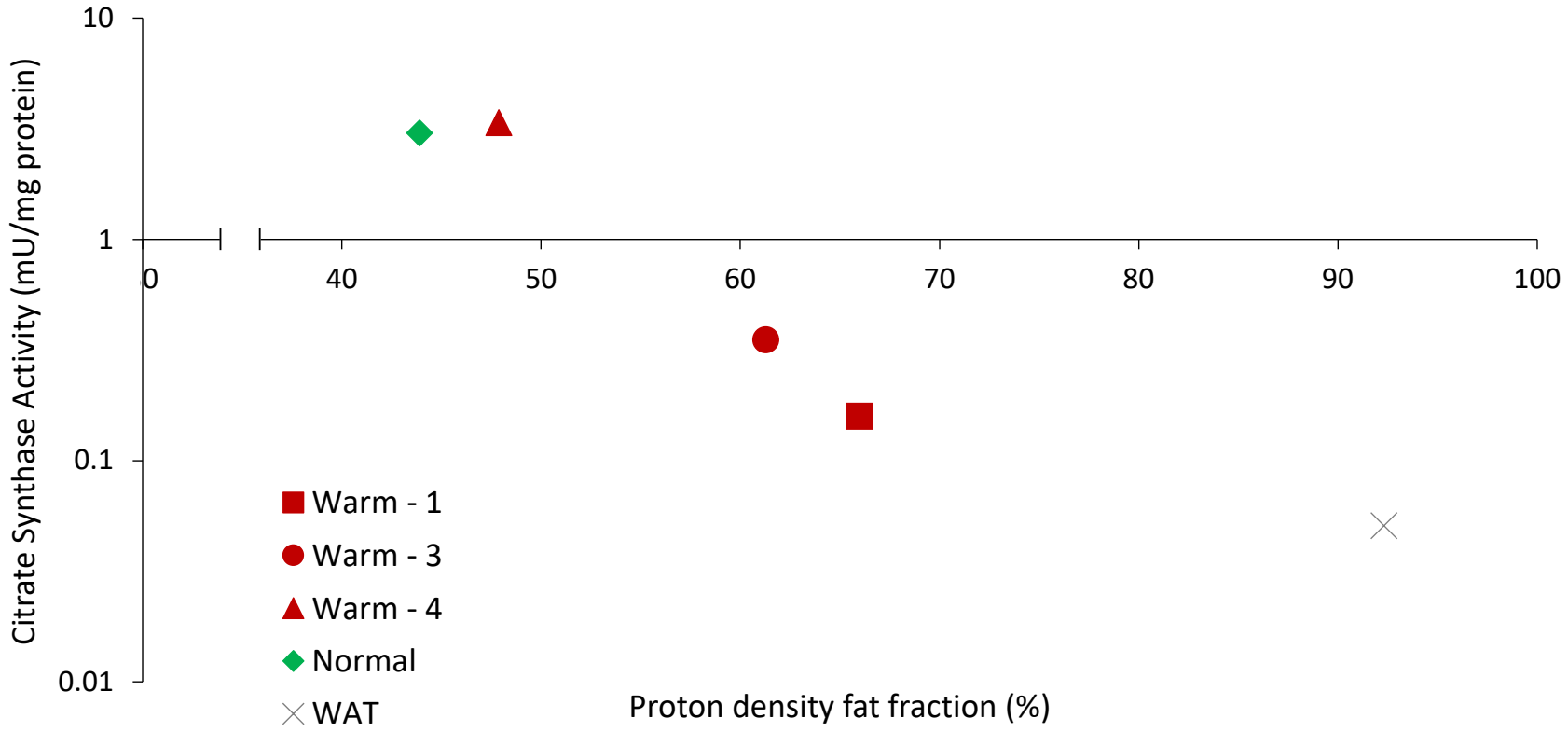

Figure 3.8 Relationship between citrate synthase activity in warm-housed animals and proton density fat fraction (PDFF). Log scale correlation between non-uniform BAT (Warm-1 and Warm-3), uniform BAT (Warm-4), a hibernating animal (animal housed at 22°C until October and then housed at 5°C until March) and WAT from a hibernator related to their respective PDFF values, r=-0.946, P<0.005.

The orbital fat depot of both cold and warm-housed animals started at 0.2±0.0ml in late August and increased in size 2.5-fold in both groups by early November (Figure 3.9A). The depot size plateaued at 0.5±0.0ml from November until early February before a 1.6-fold decrease where the depot plateaus at 0.3±0.0ml in May. After a calendar year, the depots were 0.4±0.0ml in both groups, 2.25-fold above the original volume in August 2016 when the animals were juveniles. The same pattern was seen when the orbital fat was corrected for body mass (data not shown). The orbital fat PDFF (mean 43.9±0.3%) did not differ significantly between groups ($F_{(1, 6)}$=0.3, P=0.582), and there is no interaction between time and temperature ($F_{(2.6, 15.5)}$=1.5, P=0.257) throughout the year (Figure 3.9B).

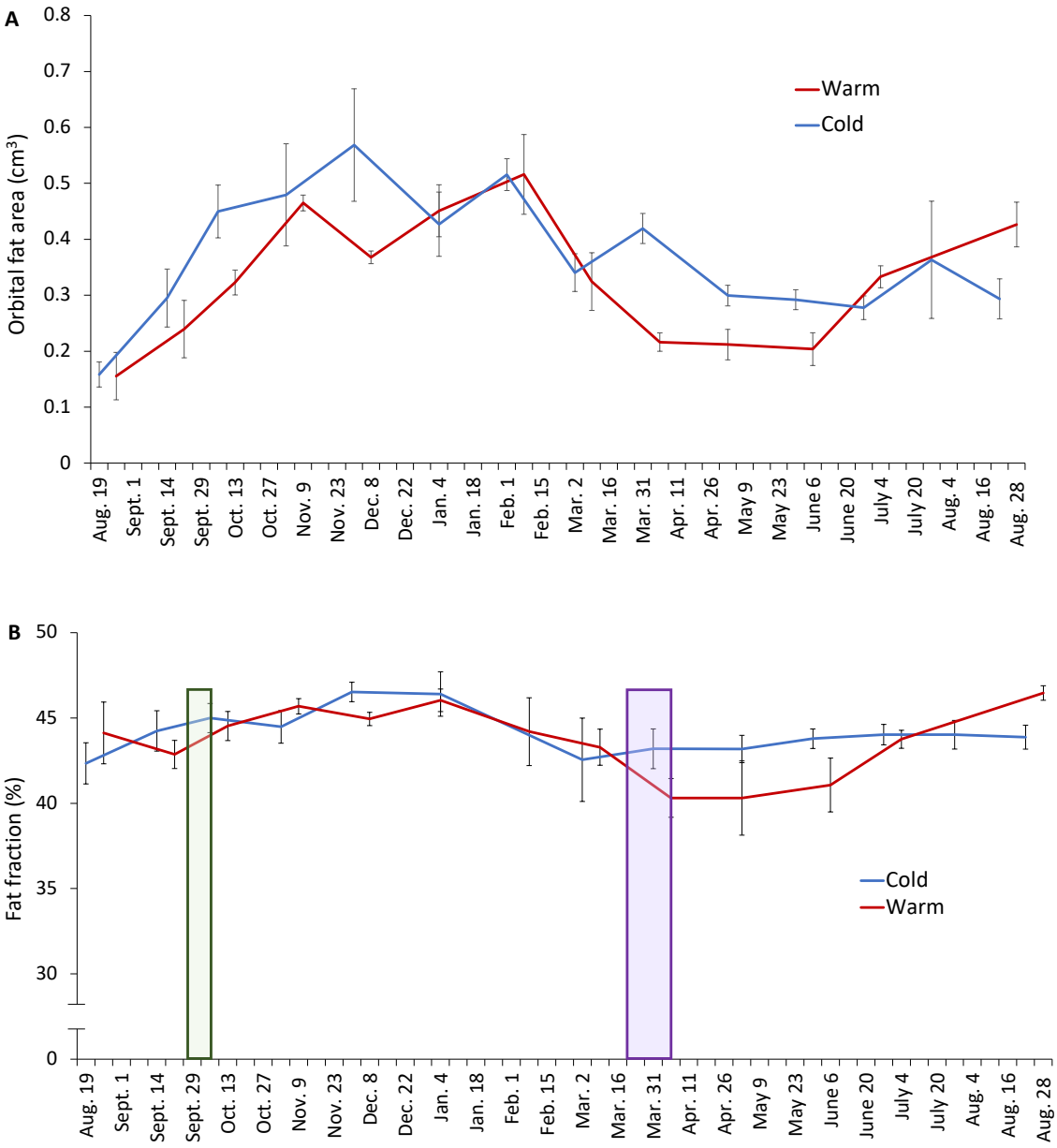

Figure 3.9 Orbital fat volume throughout one year (A) and corresponding proton density fat fraction (PDFF) (B). The red line represents animals housed at 25°C and the blue line represents animals housed at 5°C, both groups had a 12h L:12h D photoperiod. Data are presented as mean±SEM, *n*=4 for each group. The green box indicates the range of initial torpor bouts for cold-housed animals (beginning 28 September 2016). The purple box indicates the range of terminal arousals (18 March - 3 April 2017). There is a significant effect of time ($F_{(3.0, 18.1)}$=10.9, P<0.000), no significant effect of temperature ($F_{(1, 6)}$=1.6, P=0.247) or interaction between time and temperature ($F_{(3.0, 18.1)}$=2.4, P=0.105) on the orbital fat volume. There is a significant effect of time ($F_{(2.6, 15.5)}$=3.6, P=0.041), no significant effect of temperature ($F_{(1, 6)}$=0.3, P=0.582) or interaction between time and temperature ($F_{(2.6, 15.5)}$=1.5, P=0.257) on the PDFF of the orbital fat.

Contrary to my prediction, immunoblots did not detect UCP1 in the ground squirrel orbital fat. In ground squirrel Harderian gland, heart ventricle or forebrain no UCP1 was detected (Figure 3.10A), but saturating levels were observed in BAT. In addition, I did not detect UCP3 in the ground squirrel orbital fat, heart or BAT, but UCP3 protein was apparent in the Harderian gland and skeletal muscle (Figure 3.10B). In the Harderian gland proteins reacting with the UCP3 antibody had calculated molecular weights of 49kDa and 25kDa, whereas the gastrocnemius muscle had a single band at 33kDa, at the expected molecular weight for this protein in rabbit (Abcam ab10985). The difference in apparent UCP3 molecular weight between the Harderian gland and skeletal muscle could be due to a difference in UCP3 size between the two tissues, post-translational modifications of the Harderian gland protein, or non-specific binding of the rabbit-derived antibody with non-UCP3 ground squirrel proteins.

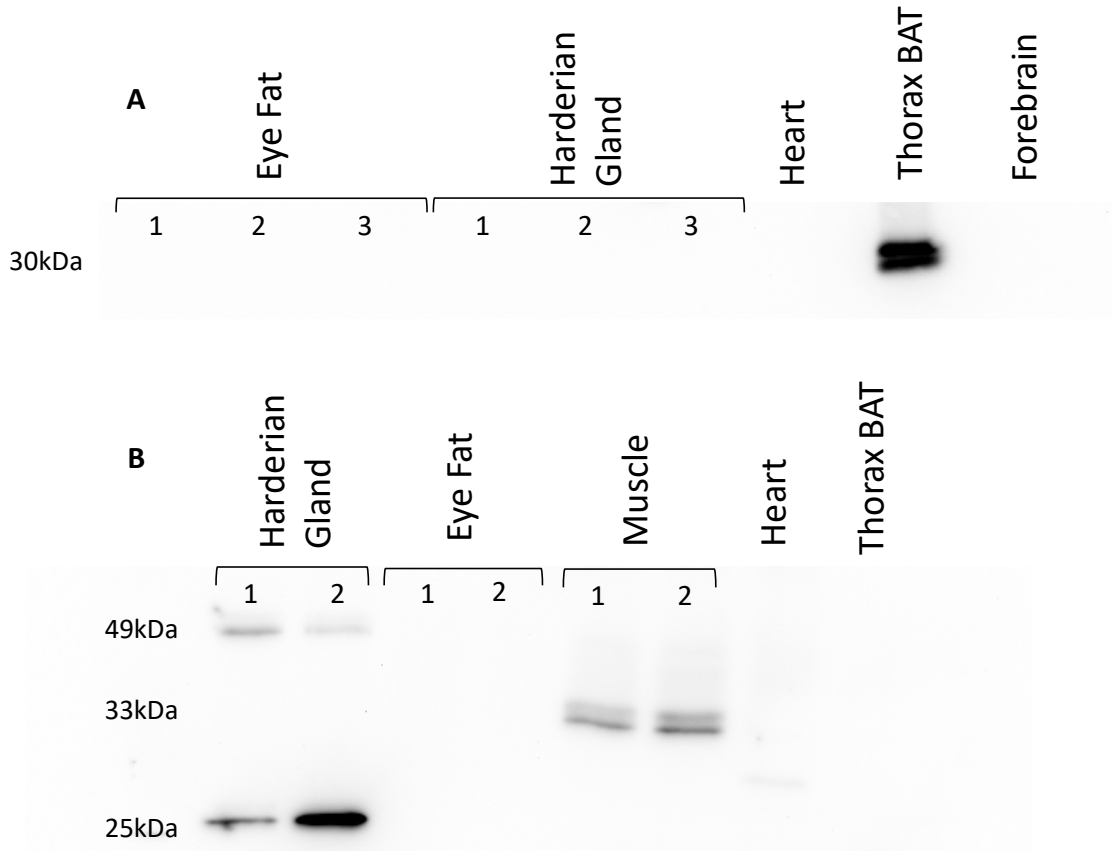

Figure 3.10 Immunoblots of uncoupling protein-1 (UCP1) (A) and uncoupling protein-3 (B). Immunoblots for UCP1 resulted in a single band for only thorax BAT at 30kDa. Immunoblots for UCP3 resulted in bands for the Harderian gland at 49kDa and muscle at 33kDa.

Hematoxylin and Eosin staining showed brown adipocytes with the typical pattern of multiple small lipid droplets whereas white adipocytes had a single, large lipid droplet, with no apparent difference between visceral and subcutaneous WAT (data not shown). In contrast, the Harderian gland had substantially larger nuclei, a typical characteristic (Aldana Marcos and Affanni, 2005) and no obvious lipid droplets (Figure 3.11). The orbital fat appears to have multi-layered cuboidal epithelial cells surrounding what appear to be blood vessels. The histological properties are distinct among the four tissues and suggest that orbital fat depot is neither WAT, BAT nor Harderian gland.

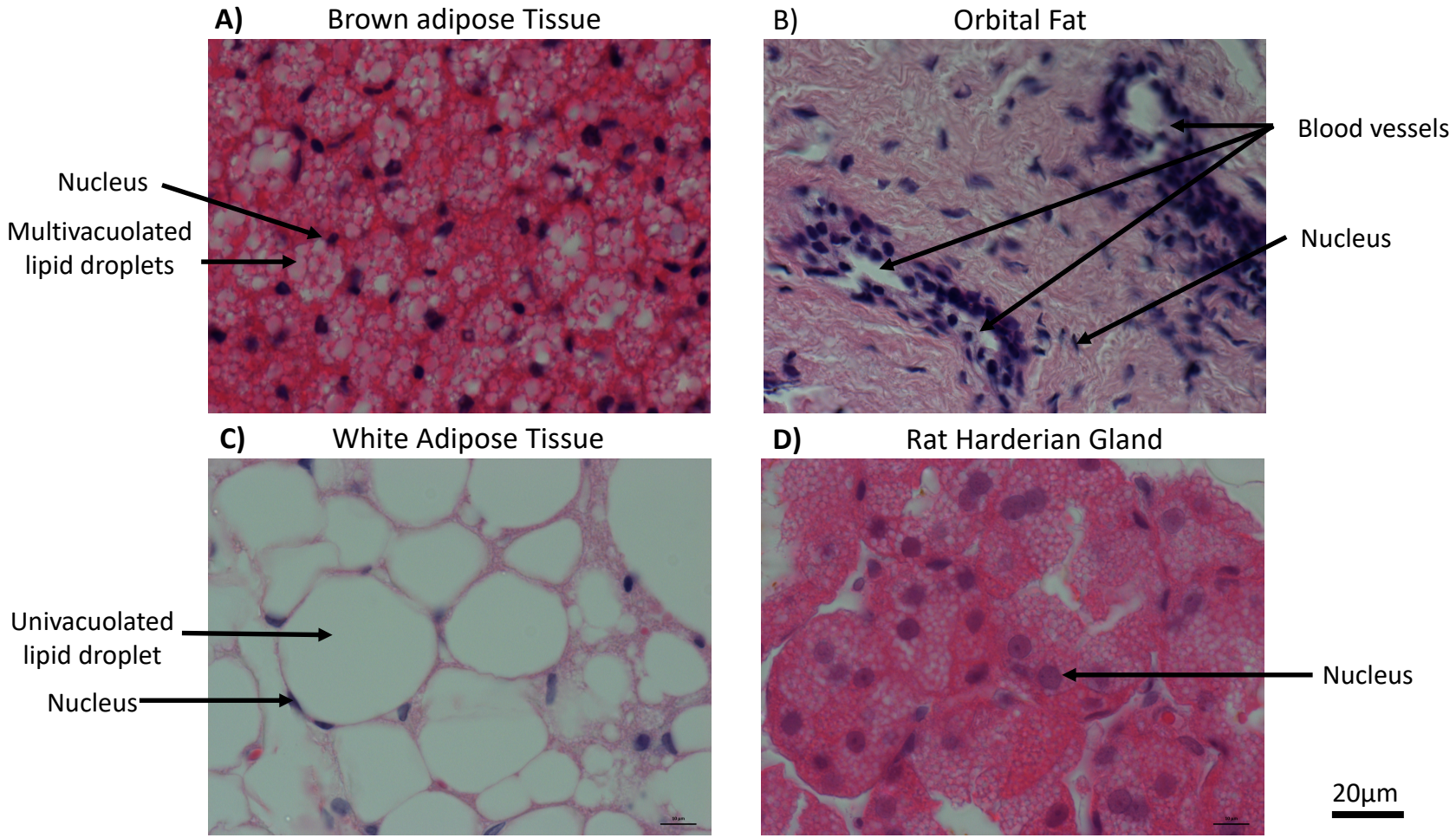

Figure 3.11 Hematoxylin & Eosin stained tissues. Tissues were formalin fixed and paraffin embedded. Sectioning shows distinct variations in histology of the tissues. All photomicrographs are shown with the same magnification, all images were taken at the same magnification (40x).

Chapter 4

4 Discussion

Although the 13-lined ground squirrel is considered to be an obligate hibernator, my findings suggest that these animals are actually facultative hibernators. The 13-lined ground squirrel does have an endogenous circannual rhythm of BAT but not body mass or WAT volume. The PDFF of visceral WAT decreased during the winter months in the cold-housed animals but not the warm-housed animals. The orbital fat pad does not express UCP1 or have histological features of BAT and is therefore not likely BAT but possibly a vascular rete.

4.1 Circannual Patterns

Since 13-lined ground squirrels are thought to be obligate hibernators I hypothesized that body mass, WAT and BAT volume would show an endogenous circannual rhythm. Contrary to my hypothesis there is no evidence of an endogenous rhythm of body mass or WAT volume. The differences in body mass gain and loss between the warm and cold-housed animals differ from the golden-mantled ground squirrel, which demonstrates a strict endogenous rhythm of body mass regardless, T_a or photoperiod (Pengelley and Asmundson, 1969, Florant et al., 2012). The greatest contributor to mass change in most mammals is WAT. The % body mass composed of WAT was as high as 56.7% in the 13-lined ground squirrel (Figure 3.2). This is much higher than in non-hibernating mice, where WAT typically contributes to 2.4% of body mass, and only increases to 22.7% when fed high calorie, high fat diets (Sjögren et al., 2001). However, in my study WAT volume decreased in the warm group from February to April, but this change was not reflected in total body mass. Changes in body mass did reflect changes in WAT volume in a previous experiment where 13-lined ground squirrels were housed with photoperiod mimicking Carman MB, and a temperature of ~20°C until October and 5°C during the winter months (MacCannell et al., 2017). The difference between these two studies suggests that WAT dynamics are not regulated solely by an endogenous rhythm, and T_a and photoperiod may serve as zeitgebers.

WAT does not appear to be the main contributor to mass gain in warm-housed animals during the winter and spring, which could be related to demonstrated patterns of protection against muscle atrophy. Hibernating mammals have restricted muscle movements during the winter months since they spend the majority of their time in torpor. Despite this relative inactivity, prairie dogs and bears conserve skeletal muscle mass and protein content in anticipation for hibernation (Cotton and Harlow, 2010), though the mechanism underlying this phenomenon is not fully understood. It is possible that the disconnect between body mass and WAT volume in the warm-housed ground squirrels arose because these animals did not hibernate during the winter. These animals fed and maintained some physical activity, which together may have augmented mechanisms that prevent muscle atrophy in the winter. As a result, although WAT volume declined, body mass did not, perhaps because skeletal muscle mass represented a larger proportion of total animal mass, compared with the cold-housed animals. By contrast the inactive, fasting, cold-housed animals likely used muscle sparing mechanisms simply to defend against atrophy (Andres-Mateos et al., 2012), and muscle mass is not as large of a contributor to total mass changes as WAT. To determine if this is the case, the MRI data collected could be used to determine if there is a change in muscle volume between the cold and warm groups during the winter and spring, where I see the disconnect between WAT and body mass. Some preliminary data from our lab (C.F. Watt, J.F. Staples and A.D.V. MacCannell, unpublished data) also suggest that there may be an increase in the liver and heart volumes within the cold-housed squirrels, which may also contribute to increased mass in the spring that is not explained by changes in WAT.

The increase in BAT volume during early fall in both cold and warm groups agrees with my recent observation (MacCannell et al., 2017) that BAT growth can occur in a hibernator in the absence of cold exposure. In fact, the largest increase in BAT volume was found shortly after MRI began in the late summer in the animals housed at thermoneutral temperature. Even in the subsequent spring these warm animals showed a greater increase in BAT volume than their cold counterparts. This pattern suggests that BAT has an endogenous rhythm of depot increase in the fall months (August – October) and decrease in late winter (February – April). These results differ from non-hibernating

mammals, where BAT depot growth results from either a decrease in T_a (Nakamura and Morrison, 2007) or high-calorie diets (Rothwell and Stock, 1979).

In non-hibernating mammals, reduced T_a stimulates the sympathetic nervous system, releasing norepinephrine. Norepinephrine binds to a brown adipocyte membrane receptor, causing a signal cascade that releases free fatty acids from triglycerides. These fatty acids are transported across the outer mitochondrial membrane and they activate UCP1. Long term simulation by norepinephrine increases transcription of the gene that encodes UCP1, therefore increasing the BAT depot and thermogenic capacity (Cannon and Nedergaard, 2004). In hibernators the BAT depot increases in volume without cold stimulation, indicating that either there is a different trigger activating the norepinephrine cascade or a separate signal altogether stimulating BAT growth. To determine if norepinephrine is involved in the depot size increase, one could transect the sympathetic nerve leading to the BAT and measure BAT depot size throughout the year. If the BAT continues to show a circannual pattern of growth this would indicate that a separate phenomenon is causing the observed volume changes of BAT in hibernators without cold exposure. Determining the level of circulating hormone through cannulation of the animals would also allow for further determination of the effects of norepinephrine on the adipose changes of these animals.

Overall data from this study suggests that the 13-lined ground squirrel is not an obligate hibernator. Daily inspection of the animals housed at a thermoneutral 25°C (Long et al., 2005, Vispo and Bakken, 1993) showed no indications of torpor. In a separate study I confirmed this observation with radio telemeters implanted in animals housed at a thermoneutral 25°C and 12h L:12h D. Preliminary data from one animal shows only three instances of T_b dropping below 30°C, with the longest decrease in temperature lasting no more than 16 hours (Appendix C).

4.2 Environmental temperature effects at the tissue level

PDFF reflects the relative amount of lipid within an entire tissue. The PDFF values of the visceral and subcutaneous WAT were within the range reported for mammalian WAT, but I did not expect the higher values in visceral depots, compared to subcutaneous. To

my knowledge such a difference is novel among mammals. For example, in humans both visceral and subcutaneous PDFF are approximately 89.7% (Franz et al., 2017). The warm animals did not enter torpor, and the difference between visceral and subcutaneous WAT was maintained throughout the year. On the other hand, the cold-housed animals repeatedly cycled between torpor and IBE and the PDFF in the visceral adipose tissue decreased to the same level as the subcutaneous adipose tissue during the hibernating months. Metabolism during both torpor and IBE is fueled predominately by lipid oxidation (reviewed by Staples, 2016). If the visceral WAT is oxidized preferentially during torpor and IBE this would account for not only the decreased lipid storage (i.e. tissue volume) in the winter, but also the decline in visceral PDFF. This pattern would suggest that visceral adipose is used for energy storage and subcutaneous adipose would be maintained to serve as thermal insulation. Once the cold-housed animals emerge from torpor and begin eating, lipid vesicles of visceral WAT likely replenish their TAG stores, leading to an increase in both PDFF and WAT volume. By contrast the warm-housed squirrels ate throughout the entire hibernation season, so the PDFF of WAT did not change throughout the year.

The functional differences between visceral and subcutaneous adipose in hibernators that I propose has some support from research on humans. Humans exhibit metabolic differences between visceral and subcutaneous adipose tissue (Linder et al., 2004). Visceral adipocytes are smaller but more metabolically active than subcutaneous adipocytes (Ramis et al., 2002). Visceral adipose tissue has a stronger response to cateocholamine-induced lipolysis and releases glycerol three times faster than subcutaneous adipose tissue (Ostman et al., 1979). Visceral adipocytes are also less sensitive to anti-lipolytic effects of insulin than subcutaneous adipocytes (Engfeldt and Arner, 1988). Since visceral adipose tissue is more metabolically active and faster at releasing glycerol than subcutaneous adipocytes, this supports my hypothesis that the lipid within the visceral adipose tissue is being broken down and used to fuel metabolism, especially during arousals over the hibernation season.

The PDFF of BAT in both cold and warm-housed animals was maintained over the course of the year between 39-48% for cold and ~43-51% for warm. The higher PDFF values derived from manual segmentation of MRIs from the two warm-housed

animals showed non-uniform BAT PDFF (Figure 3.6) which suggests the hypothesis that, when housed at continuously warm temperatures, there may be loss of BAT and invasion of WAT into the BAT depot. The data in Figures 3.7 and 3.8 support this hypothesis, showing a decrease in relative UCP1 protein content and citrate synthase activity, respectively, as BAT PDFF increases. In fact, the citrate synthase activity of thoracic BAT in the animals with the highest PDFF is very similar to that of WAT (Figure 3.8).

Many recent studies have documented WAT taking on BAT characteristics and contributing to thermogenesis when rodents are housed under long-term cold exposure (Vitali et al., 2012). This "beiging" process is believed to result from a reprogramming of white adipocytes so that they express many of the same proteins as BAT, including UCP1, while remaining otherwise molecularly distinct from both WAT and BAT (Giralt and Villarroya, 2013). While WAT can be stimulated to become 'brown-like', to my knowledge there is currently no evidence of brown adipocytes transforming into white adipocytes (Sanchez-Gurmaches and Guertin, 2014). When BAT from animals held at thermoneutrality and forced through gene expression to become "WAT-like", this leads to inflammation and cell death (Kotzbeck et al., 2018). As a result, I believe the pattern I observe (Figure 3.6) represents an invasion of WAT into a space previously occupied by BAT. This contention is reflected at a molecular level; there is a negative relationship between PDFF and content of both UCP1 and citrate synthase in this depot. Maintaining animals at thermoneutral temperatures decrease adrenergical activation of BAT (Celi, 2009), suggesting that the animals housed in warm conditions are decreasing the BAT depots due to disuse and WAT is invading the space.

4.3 Orbital lipid depot

My earlier research discovered a fat depot near the eye of 13-lined ground squirrels with a similar fat fraction as BAT (MacCannell et al., 2017). During arousal, thermal images show that this area is substantially warmer than other parts of the head (Appendix A). Taken together these observations led me to hypothesize that this lipid depot was, in fact, BAT. The volume of this depot did follow a circannual pattern similar to BAT volume (Figures 3.5A and 3.9A). However, data in this thesis has led me to conclude that this tissue is not BAT. This tissue does not express either UCP1 or UCP3 (Figure 3.10) and

histologically it does not resemble BAT. Nonetheless these observations allow me to speculate on the nature of this tissue.

The histology shows blood vessels in close apposition to each other, a similar pattern to circulatory retes. Retes utilize counter current heat exchange with blood vessels in close proximity to each other which flow in opposite directions (Cech et al., 1984). Such organs are found within several different taxa including birds, fish and mammals, even near the eyes and optic sinuses of salmon shark (*Lamna ditropis*) and big eye thresher shark (*Alopias superciliosus*), where they function as a vascular heat exchanger, maintaining higher temperatures than other tissues (Cech et al., 1984, Weng and Block, 2004). Many aquatic mammals (lamnid sharks, bill-fishes, tunas and opah) have independently developed structures behind their eyes that can produce and retain heat, without UCP1 but through extra ocular muscles and vascular heat exchange systems (Runcie et al., 2009, Block and Carey, 1985, Carey, 1982, Block, 1991). The rete size of the bigeye thresher shark varies by season (Weng and Block, 2004), which is similar to the seasonal pattern that I observed (Fig 3.9A).

Thirteen-lined ground squirrels hibernate underground in burrows with low T_a. BAT plays a large role in the re-warming process during arousals, but BAT is concentrated in the thorax region and therefore would be advantageous to restrict heat loss occurring through the fluid-filled and poorly insulated eyes, while heating up the brain during an arousal. A rete would allow blood warmed by thoracic BAT to transfer heat to cold blood returning from the periphery of the head, maintaining the temperature of the head at relatively high levels. The brain plays a major role in regulating changes to T_b, metabolism and physiological variables, so rewarming of the brain before other tissues would be advantageous to the arousal process (Heller and Colliver, 1974, Dark et al., 1990).

4.4 Conclusions and Future directions

My data suggests that the 13-lined ground squirrel is not a typical obligate hibernator. This species does not have an endogenous rhythm of WAT volume or body mass. Both the body mass and WAT volume in the warm-housed animals was significantly higher than the cold-housed animals during the winter months. The animals did, however, show

suggestions of a circannual pattern of BAT volume. Although the WAT volume might not have an endogenous rhythm it is vital for fuelling metabolism, especially during arousals, as shown by the decrease in PDFF of animals hibernating in the cold treatment.

Future work should confirm the circannual patterns I observed by extending this project from one year to multiple years, as done in previous studies of obligate hibernators such as the golden-mantled ground squirrel. I am working towards clarifying the effect of T_a on hibernation patterns in this species using T_b loggers implanted within ground squirrels housed at 12h L:12h D and either 25°C, 16°C or 5°C. I hypothesize that animals housed at higher temperatures (25°C or 16°C) will not enter torpor (T_b less than 30°C), showing that environmental temperature is a necessary cue for hibernation in the 13-lined ground squirrel.

My investigations suggest that the orbital fat deposit is neither BAT nor Harderian gland, but resembles a vascular rete, at least at the histological level. To determine the vascular nature of the orbital fat histological staining for vascular adhesion molecules (e.g. PECAM-1, VCAM-1) (Haraldsen et al., 1996, Albelda, 1991, Albelda et al., 1991) since they are specific markers for blood vessels. The nature of the high proton density fat fraction of the orbital depot remains unknown. Further characterization of these lipids by NMR would identify types of lipids, offering clues to the nature of this tissue. Gene expression analysis would give an overarching idea of functional genes within the orbital fat, providing more information about this tissue's phenotype.

References

Albelda, S.M. (1991). Endothelial and epithelial cell adhesion molecules. Am J Respir Cell Mol Biol *4*, 195–203.

Albelda, S.M., Muller, W.A., Buck, C.A., and Newman, P.J. (1991). Molecular and cellular properties of PECAM-1 (endoCAM/CD31): a novel vascular cell-cell adhesion molecule. J. Cell Biol. *114*, 1059–1068.

Aldana Marcos, H.J., and Affanni, J.M. (2005). Anatomy, histology, histochemistry and fine structure of the Harderian gland in the South American armadillo Chaetophractus villosus (Xenarthra, Mammalia). Anat. Embryol. (Berl.) *209*, 409–424.

Andreani, T.S., Itoh, T.Q., Yildirim, E., Hwangbo, D.-S., and Allada, R. (2015). Genetics of Circadian Rhythms. Sleep Med. Clin. *10*, 413–421.

Andres-Mateos, E., Mejias, R., Soleimani, A., Lin, B.M., Burks, T.N., Marx, R., Lin, B., Zellars, R.C., Zhang, Y., Huso, D.L., et al. (2012). Impaired skeletal muscle regeneration in the absence of fibrosis during hibernation in 13-lined ground squirrels. PloS One *7*, e48884.

Aschoff, J. (1981). A Survey on Biological Rhythms. In Biological Rhythms, (Springer, Boston, MA), pp. 3–10.

Ballinger, M.A., Hess, C., Napolitano, M.W., Bjork, J.A., and Andrews, M.T. (2016). Seasonal Changes in Brown Adipose Tissue Mitochondria in a Mammalian Hibernator: from Gene Expression to Function. Am. J. Physiol. Regul. Integr. Comp. Physiol. ajpregu.00463.2015.

Barger, J.L., Barnes, B.M., and Boyer, B.B. (2006). Regulation of UCP1 and UCP3 in arctic ground squirrels and relation with mitochondrial proton leak. J. Appl. Physiol. *101*, 339–347.

Block, B.A. (1991). Endothermy in fish: thermogenesis, ecology and evolution. In Biochemistry and Molecular Biology of Fishes, (Elsevier), pp. 269–311.

Block, B.A., and Carey, F.G. (1985). Warm brain and eye temperatures in sharks. J. Comp. Physiol. [B] *156*, 229–236.

Boushel, R., Gnaiger, E., Schjerling, P., Skovbro, M., Kraunsøe, R., and Dela, F. (2007). Patients with type 2 diabetes have normal mitochondrial function in skeletal muscle. Diabetologia *50*, 790–796.

Cannon, B., and Nedergaard, J. (2004). Brown Adipose Tissue: Function and Physiological Significance. Physiol. Rev. *84*, 277–359.

Carey, F.G. (1982). A brain heater in the swordfish. Science *216*, 1327–1329.

Cech, J.J., Laurs, R.M., and Graham, J.B. (1984). Temperature-Induced Changes in Blood Gas Equilibria in the Albacore, Thunnus Alalunga, a Warm-Bodied Tuna. J. Exp. Biol. *109*, 21–34.

Celi, F.S. (2009). Brown Adipose Tissue — When It Pays to Be Inefficient. N. Engl. J. Med. *360*, 1553–1556.

Chayama, Y., Ando, L., Tamura, Y., Miura, M., and Yamaguchi, Y. (2016). Decreases in body temperature and body mass constitute pre-hibernation remodelling in the Syrian golden hamster, a facultative mammalian hibernator. R. Soc. Open Sci. *3*.

Contreras, C., Nogueiras, R., Diéguez, C., Medina-Gómez, G., and López, M. (2016). Hypothalamus and thermogenesis: Heating the BAT, browning the WAT. Mol. Cell. Endocrinol. *438*, 107–115.

Cotton, C.J., and Harlow, H.J. (2010). Avoidance of skeletal muscle atrophy in spontaneous and facultative hibernators. Physiol. Biochem. Zool. PBZ *83*, 551–560.

Dark, J., Pikard, Gerye, and Zucker, Irving (1984). Persistence of circannual rhythms in ground squirrels with lesions of the suprachiasmatic nuclei. Brain Res. *332*, 201–207.

Dark, J., Kilduff, T.S., Heller, H.C., Licht, P., and Zucker, I. (1990). Suprachiasmatic nuclei influence hibernation rhythms of golden-mantled ground squirrels. Brain Res. *509*, 111–118.

Drew, K.L., Buck, C.L., Barnes, B.M., Christian, S.L., Rasley, B.T., and Harris, M.B. (2007). Central nervous system regulation of mammalian hibernation: implications for metabolic suppression and ischemia tolerance. J. Neurochem. *102*, 1713.

Dupré, S.M., and Loudon, A.S.I. (2007). Circannual Clocks: Annual Timers Unraveled in Sheep. Curr. Biol. *17*, R216–R217.

Engfeldt, P., and Arner, P. (1988). Lipolysis in human adipocytes, effects of cell size, age and of regional differences. Horm. Metab. Res. Suppl. Ser. *19*, 26–29.

Espeland, A., Vetti, N., and Kråkenes, J. (2013). Are two readers more reliable than one? A study of upper neck ligament scoring on magnetic resonance images. BMC Med. Imaging *13*, 4.

Feist et al. (1985). Regulation of energy stores in arctic ground squirrels: Brown fat thermogenic capacity, lipoprotein lipase and pancreatic hormones during fat deposition. In Living in the Cold: Physiological and Biochemical Adaptations, (Elsevier Science Publishing Co., Inc.), pp. 281–285.

Florant, G.L., Richter, M.M., and Fried, S.K. (2012). The Effect of Ambient Temperature on Body Mass, Torpor, Food Intake, and Leptin Levels: Implications on the Regulation of Food Intake in Mammalian Hibernators. In Living in a Seasonal World, T. Ruf, C. Bieber, W. Arnold, and E. Millesi, eds. (Springer Berlin Heidelberg), pp. 507–517.

Franz, D., Weidlich, D., Freitag, F., Holzapfel, C., Drabsch, T., Baum, T., Eggers, H., Witte, A., Rummeny, E.J., Hauner, H., et al. (2017). Association of proton density fat fraction in adipose tissue with imaging-based and anthropometric obesity markers in adults. Int. J. Obes.

Fuller, S., Reeder, S., Shimakawa, A., Yu, H., Johnson, J., Beaulieu, C., and Gold, G.E. (2006). Iterative Decomposition of Water and Fat with Echo Asymmetry and Least-Squares Estimation (IDEAL) Fast Spin-Echo Imaging of the Ankle: Initial Clinical Experience. Am. J. Roentgenol. *187*, 1442–1447.

Giralt, M., and Villarroya, F. (2013). White, Brown, Beige/Brite: Different Adipose Cells for Different Functions? Endocrinology *154*, 2992–3000.

Hampton, M., Melvin, R.G., and Andrews, M.T. (2013). Transcriptomic Analysis of Brown Adipose Tissue across the Physiological Extremes of Natural Hibernation. PLOS ONE *8*, e85157.

Haraldsen, G., Kvale, D., Lien, B., Farstad, I.N., and Brandtzaeg, P. (1996). Cytokine-regulated expression of E-selectin, intercellular adhesion molecule-1 (ICAM-1), and vascular cell adhesion molecule-1 (VCAM-1) in human microvascular endothelial cells. J. Immunol. *156*, 2558–2565.

Hardin, P.E., Hall, J.C., and Rosbash, M. (1990). Feedback of the Drosophila period gene product on circadian cycling of its messenger RNA levels. Nature *343*, 536–540.

Hardin, P.E., Hall, J.C., and Rosbash, M. (1992). Circadian oscillations in period gene mRNA levels are transcriptionally regulated. Proc. Natl. Acad. Sci. U. S. A. *89*, 11711–11715.

Hauenschild, C. (1960). Lunar Periodicity. Cold Spring Harb. Symp. Quant. Biol. *25*, 491–497.

Heller, H.C., and Colliver, G.W. (1974). CNS regulation of body temperature during hibernation. Am. J. Physiol.-Leg. Content *227*, 583–589.

Henshaw, R.E., Underwood, L.S., and Casey, T.M. (1972). Peripheral thermoregulation: foot temperature in two Arctic canines. Science *175*, 988–990.

Herrington, L.P. (1951). The role of the piliary system in mammals and its relation to the thermal environment. Ann. N. Y. Acad. Sci. *53*, 600–607.

Herzog, E.D. (2007). Neurons and networks in daily rhythms. Nat. Rev. Neurosci. *8*, 790–802.

Hindle, A.G., and Martin, S.L. (2014). Intrinsic circannual regulation of brown adipose tissue form and function in tune with hibernation. Am. J. Physiol.-Endocrinol. Metab. *306*, E284–E299.

Hines, C.D.G., Yu, H., Shimakawa, A., McKenzie, C.A., Warner, T.F., Brittain, J.H., and Reeder, S.B. (2010). Quantification of hepatic steatosis with 3-T MR imaging: validation in ob/ob mice. Radiology *254*, 119–128.

Hoffmann, U., Brix, G., Scharf, J., and Lorenz, W.J. (1997). Quantitative analysis of the portal and arterial blood supply of liver lesions by means of dynamic MRI. In Proc Int Soc Magn Reson Med, (Wiley Online Library), p. 2083.

Hu, H.H., Smith, D.L., Nayak, K.S., Goran, M.I., and Nagy, T.R. (2010). Identification of Brown Adipose Tissue in Mice with Fat-Water IDEAL-MRI. J. Magn. Reson. Imaging JMRI *31*, 1195–1202.

Humphries, M.M., Thomas, D.W., and Kramer, D.L. (2003). The Role of Energy Availability in Mammalian Hibernation: A Cost-Benefit Approach. Physiol. Biochem. Zool. *76*, 165–179.

King, D.P., and Takahashi, J.S. (2000). Molecular genetics of circadian rhythms in mammals. Annu. Rev. Neurosci. *23*, 713–742.

Kisser, B., and Goodwin, H.T. (2012). Hibernation and Overwinter Body Temperatures in Free-Ranging Thirteen-Lined Ground Squirrels, Ictidomys tridecemlineatus. Am. Midl. Nat. *167*, 396–409.

Kotzbeck, P., Giordano, A., Mondini, E., Murano, I., Severi, I., Venema, W., Cecchini, M.P., Kershaw, E.E., Barbatelli, G., Haemmerle, G., et al. (2018). Brown adipose tissue whitening leads to brown adipocyte death and adipose tissue inflammation. J. Lipid Res.

Laske, T.G., Harlow, H.J., Garshelis, D.L., and Iaizzo, P.A. (2010). Extreme respiratory sinus arrhythmia enables overwintering black bear survival--physiological insights and applications to human medicine. J Cardiovasc. Transl. Res. *3*, 559–569.

Laursen, W.J., Mastrotto, M., Pesta, D., Funk, O.H., Goodman, J.B., Merriman, D.K., Ingolia, N., Shulman, G.I., Bagriantsev, S.N., and Gracheva, E.O. (2015). Neuronal UCP1 expression suggests a mechanism for local thermogenesis during hibernation. Proc. Natl. Acad. Sci. U. S. A. *112*, 1607–1612.

Lincoln, G.A., Clarke, I.J., Hut, R.A., and Hazlerigg, D.G. (2006). Characterizing a mammalian circannual pacemaker. Science *314*, 1941–1944.

Linder, K., Arner, P., Flores-Morales, A., Tollet-Egnell, P., and Norstedt, G. (2004). Differentially expressed genes in visceral or subcutaneous adipose tissue of obese men and women. J. Lipid Res. *45*, 148–154.

Long, R.A., Martin, T.J., and Barnes, B.M. (2005). Body Temperature and Activity Patterns in Free-Living Arctic Ground Squirrels. J. Mammal. *86*, 314–322.

Lowry, O.H., Rosebrough, N.J., Farr, A.L., and Randall, R.J. (1951). Protein measurement with the Folin phenol reagent. J. Biol. Chem. *193*, 265–275.

MacCannell, A., Sinclair, K., Friesen-Waldner, L., McKenzie, C.A., and Staples, J.F. (2017). Water–fat MRI in a hibernator reveals seasonal growth of white and brown adipose tissue without cold exposure. J. Comp. Physiol. B *187*, 759–767.

Maywood, E.S., O'Neill, J., Wong, G.K.Y., Reddy, A.B., and Hastings, M.H. (2006). Circadian timing in health and disease. Prog. Brain Res. *153*, 253–269.

Mogensen, M., Bagger, M., Pedersen, P.K., Fernström, M., and Sahlin, K. (2006). Cycling efficiency in humans is related to low UCP3 content and to type I fibres but not to mitochondrial efficiency. J. Physiol. *571*, 669–681.

Moore, R.Y. (1983). Organization and function of a central nervous system circadian oscillator: the suprachiasmatic hypothalamic nucleus. Fed. Proc. *42*, 2783–2789.

Moore, R.Y., Speh, J.C., and Leak, R.K. (2002). Suprachiasmatic nucleus organization. Cell Tissue Res. *309*, 89–98.

Nakamura, K., and Morrison, S.F. (2007). Central efferent pathways mediating skin cooling-evoked sympathetic thermogenesis in brown adipose tissue. Am. J. Physiol.-Regul. Integr. Comp. Physiol. *292*, R127–R136.

Nizielski, S.E., Billington, C.J., and Levine, A.S. (1989). Brown fat GDP binding and circulating metabolites during hibernation and arousal. Am. J. Physiol.-Regul. Integr. Comp. Physiol. *257*, R536–R541.

Oelkrug, R., Polymeropoulos, E.T., and Jastroch, M. (2015). Brown adipose tissue: physiological function and evolutionary significance. J. Comp. Physiol. B *185*, 587–606.

Ostman, J., Arner, P., Engfeldt, P., and Kager, L. (1979). Regional differences in the control of lipolysis in human adipose tissue. Metabolism. *28*, 1198–1205.

Payne, A.P. (1994). The harderian gland: a tercentennial review. J. Anat. *185*, 1–49.

Pengelley, E.T., and Asmundson, S.M. (1969). Free-running periods of endogenous circannian rhythms in the golden mantled ground squirrel, Citellus lateralis. Comp. Biochem. Physiol. *30*, 177–183.

Pengelley, E.T., and Fisher, K.C. (1961). Rhythmical arousal from hibernation in the golden-mantled ground squirrel, Citellus lateralis tescorum. Can. J. Zool. *39*, 105–120.

Pittendrigh, C.S. (1960). Circadian rhythms and the circadian organization of living systems. Cold Spring Harb. Symp. Quant. Biol. *25*, 159–184.

Prakash, K.N.B., Verma, S.K., Yaligar, J., Goggi, J., Gopalan, V., Lee, S.S., Tian, X., Sugii, S., Leow, M.K.S., Bhakoo, K., et al. (2016). Segmentation and characterization of interscapular brown adipose tissue in rats by multi-parametric magnetic resonance imaging. Magn. Reson. Mater. Phys. Biol. Med. *29*, 277–286.

Raimbault, S., Dridi, S., Denjean, F., Lachuer, J., Couplan, E., Bouillaud, F., Bordas, A., Duchamp, C., Taouis, M., and Ricquier, D. (2001). An uncoupling protein homologue putatively involved in facultative muscle thermogenesis in birds. Biochem. J. *353*, 441–444.

Ramis, J.M., Hal, N.L.W.F., Kramer, E., Llado, I., Bouillaud, F., Palou, A., and Keijer, J. (2002). Carboxypeptidase E and thrombospondin-1 are differently expressed in subcutaneous and visceral fat of obese subjects. Cell. Mol. Life Sci. CMLS *59*, 1960–1971.

Rasmussen, J.M., Entringer, S., Nguyen, A., Erp, T.G.M. van, Guijarro, A., Oveisi, F., Swanson, J.M., Piomelli, D., Wadhwa, P.D., Buss, C., et al. (2013). Brown Adipose Tissue Quantification in Human Neonates Using Water-Fat Separated MRI. PLOS ONE *8*, e77907.

Reeder, S.B., Pineda, A.R., Wen, Z., Shimakawa, A., Yu, H., Brittain, J.H., Gold, G.E., Beaulieu, C.H., and Pelc, N.J. (2005). Iterative decomposition of water and fat with echo asymmetry and least-squares estimation (IDEAL): Application with fast spin-echo imaging. Magn. Reson. Med. *54*, 636–644.

Reeder, S.B., Robson, P.M., Yu, H., Shimakawa, A., Hines, C.D.G., McKenzie, C.A., and Brittain, J.H. (2009). Quantification of hepatic steatosis with MRI: the effects of accurate fat spectral modeling. J. Magn. Reson. Imaging JMRI *29*, 1332–1339.

Refinetti, R., and Menaker, M. (1992). The circadian rhythm of body temperature. Physiol. Behav. *51*, 613–637.

Ross, R., Léger, L., Guardo, R., De Guise, J., and Pike, B.G. (1991). Adipose tissue volume measured by magnetic resonance imaging and computerized tomography in rats. J. Appl. Physiol. Bethesda Md 1985 *70*, 2164–2172.

Rothwell, N.J., and Stock, M.J. (1979). A role for brown adipose tissue in diet-induced thermogenesis. Nature *281*, 31.

Runcie, R.M., Dewar, H., Hawn, D.R., Frank, L.R., and Dickson, K.A. (2009). Evidence for cranial endothermy in the opah (Lampris guttatus). J. Exp. Biol. *212*, 461–470.

Russell, R.L., O'Neill, P.H., Epperson, L.E., and Martin, S.L. (2010). Extensive use of torpor in 13-lined ground squirrels in the fall prior to cold exposure. J. Comp. Physiol. [B] *180*, 1165–1172.

Sanchez-Gurmaches, J., and Guertin, D.A. (2014). Adipocyte lineages: Tracing back the origins of fat. Biochim. Biophys. Acta BBA - Mol. Basis Dis. *1842*, 340–351.

Scholander, P.F., Walters, V., Hock, R., and Irving, L. (1950). Body insulation of some arctic and tropical mammals and birds. Biol. Bull. *99*, 225–236.

Sheriff, M.J., Fridinger, R.W., Tøien, Ø., Barnes, B.M., and Buck, C.L. (2013). Metabolic rate and prehibernation fattening in free-living arctic ground squirrels. Physiol. Biochem. Zool. *86*, 515–527.

Sjögren, K., Hellberg, N., Bohlooly-Y, M., Savendahl, L., Johansson, M.S., Berglindh, T., Bosaeus, I., and Ohlsson, C. (2001). Body Fat Content Can Be Predicted In Vivo in Mice Using a Modified Dual-Energy X-Ray Absorptiometry Technique. J. Nutr. *131*, 2963–2966.

Staples, J.F. (2016). Metabolic flexibility: hibernation, torpor, and estivation. Compr. Physiol.

Strijkstra, A.M. (2009). Hibernation. In Encyclopedia of Neuroscience, M.D. Binder, N. Hirokawa, and U. Windhorst, eds. (Springer Berlin Heidelberg), pp. 1831–1836.

Trayhurn, P., and Beattie, J.H. (2001). Physiological role of adipose tissue: white adipose tissue as an endocrine and secretory organ. Proc. Nutr. Soc. *60*, 329–339.

Vázquez-Vela, M.E.F., Torres, N., and Tovar, A.R. (2008). White adipose tissue as endocrine organ and its role in obesity. Arch. Med. Res. *39*, 715–728.

Vispo, C.R., and Bakken, G.S. (1993). The Influence of Thermal Conditions on the Surface Activity of Thirteen-Lined Ground Squirrels. Ecology *74*, 377–389.

Vitali, A., Murano, I., Zingaretti, M.C., Frontini, A., Ricquier, D., and Cinti, S. (2012). The adipose organ of obesity-prone C57BL/6J mice is composed of mixed white and brown adipocytes. J. Lipid Res. *53*, 619–629.

Wang, L.C.H. (1979). Time patterns and metabolic rates of natural torpor in the Richardson's ground squirrel. Can. J. Zool. *57*, 149–155.

Watanabe, M. (1980). An autoradiographic, biochemical, and morphological study of the Harderian gland of the mouse. J. Morphol. *163*, 349–365.

Weng, K.C., and Block, B.A. (2004). Diel vertical migration of the bigeye thresher shark (Alopias superciliosus), a species possessing orbital retia mirabilia. Fish. Bull. *102*, 221–229.

Wilson, C.M. (1983). [18] Staining of proteins on gels: Comparisons of dyes and procedures. In Methods in Enzymology, (Elsevier), pp. 236–247.

Wronska, A., and Kmiec, Z. (2012). Structural and biochemical characteristics of various white adipose tissue depots. Acta Physiol. *205*, 194–208.

Yan, J., Burman, A., Nichols, C., Alila, L., Showe, L.C., Showe, M.K., Boyer, B.B., Barnes, B.M., and Marr, T.G. (2006). Detection of differential gene expression in brown adipose tissue of hibernating arctic ground squirrels with mouse microarrays. Physiol. Genomics *25*, 346–353.

Yu, H., Shimakawa, A., McKenzie, C.A., Brodsky, E., Brittain, J.H., and Reeder, S.B. (2008). Multi-Echo Water-Fat Separation and Simultaneous R2* Estimation with Multi-Frequency Fat Spectrum Modeling. Magn. Reson. Med. Off. J. Soc. Magn. Reson. Med. Soc. Magn. Reson. Med. *60*, 1122–1134.

Appendices

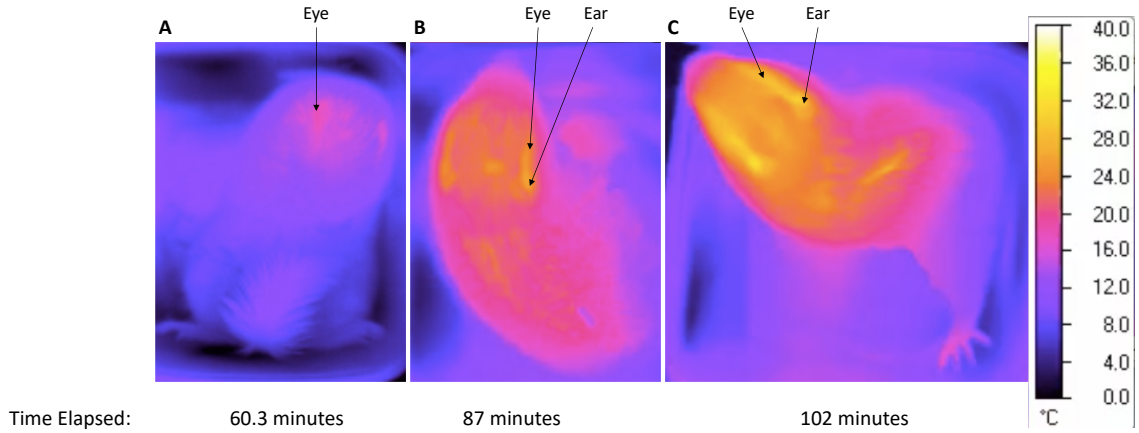

Appendix A: Thermal images of a squirrel during and induced arousal. Arrows indicate estimated locations of eyes and ear. Image A was take 60.3 minutes after the animal was removed from the hibernation chamber, image B was taken at 87 minutes and image C at 102 minutes.

Appendix B: Animal use ethics approval

2012-016::2:

AUP Number: 2012-016
AUP Title: Regulation of mitochondrial metabolism in mammalian hibernation and ageing.
Yearly Renewal Date: 08/01/2014

The YEARLY RENEWAL to Animal Use Protocol (AUP) 2012-016 has been approved, and will be approved for one year following the above review date.

1. This AUP number must be indicated when ordering animals for this project.
2. Animals for other projects may not be ordered under this AUP number.
3. Purchases of animals other than through this system must be cleared through the ACVS office.
   Health certificates will be required.

REQUIREMENTS/ COMMENTS
Please ensure that individual(s) performing procedures on live animals, as described in this protocol, are familiar with the contents of this document.

The holder of this Animal Use Protocol is responsible to ensure that all associated safety components (biosafety, radiation safety, general laboratory safety) comply with institutional safety standards and have received all necessary approvals. Please consult directly with your institutional safety officers.

Submitted by: Kinchlea, Will D
on behalf of the Animal Use Subcommittee

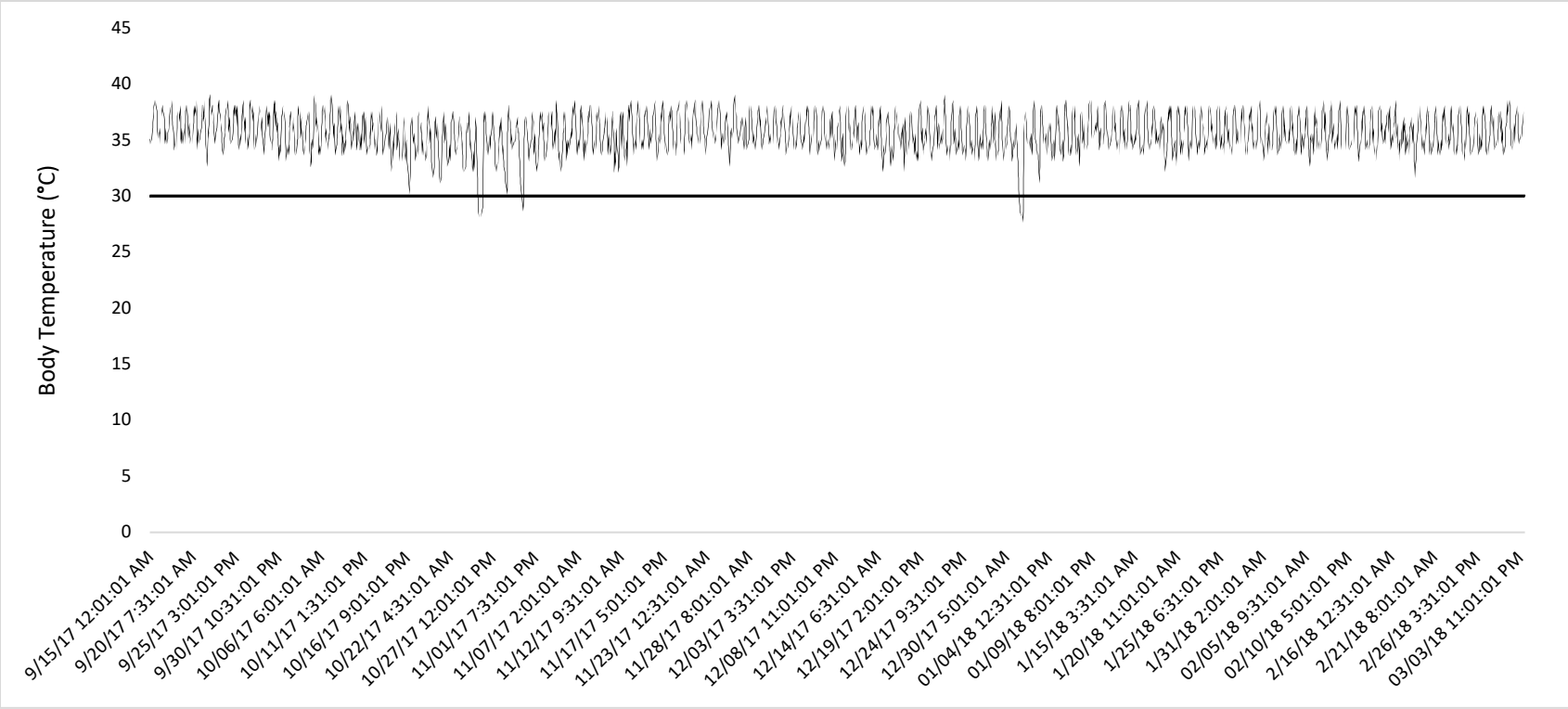

Appendix C: Internal body temperature of a single ground squirrel housed at 25°C and 12h L:12h D. A 13-lined ground squirrel was implanted with a temperature sensitive data logger which measured core body temperature every 30 minutes. The transmitter was active from 12 September 2017 to 4 March 2018. It detected three instances of temperature drop below 30°C, which is the body temperature typically used to indicate torpor.

Curriculum Vitae

Amanda MacCannell

EDUCATION

MSc Biology 2016 – present
Supervisors: Dr. James Staples and Dr. Charles McKenzie
University of Western Ontario, London, ON, Canada

BSc Honor Specialization in Genetics 2012 – 2016
University of Western Ontario, London, ON, Canada

AWARDS

Biology Conference Travel Award 2018
Peter Hochachka Symposium, best student poster 2017
NSERC USRA 2015

CONFERENCE PRESENTATIONS

MacCannell, A.D.V., Sinclair, K.J., McKenzie C.A., and Staples, J.F. Environmental temperature effects on adipose tissue in a mammalian hibernator, the 13-lined ground squirrel. Oral presentation delivered at Society for Experimental Biology, Florence, Italy, July 2018.

MacCannell, A.D.V., Sinclair, K.J., McKenzie C.A., and Staples, J.F. Using water-fat MRI to detect remodeling of adipose tissue. Poster presentation delivered at the International Society for Magnetic Resonance in Medicine, Paris, France, June 2018.

MacCannell, A.D.V., Sinclair, K.J., Friesen-Waldner L.J., McKenzie C.A., and Staples, J.F. Endogenous rhythms of thorax brown adipose tissue in the 13-lined ground squirrel. Poster presentation delivered at the Peter Hochachka Symposium, Winnipeg, MB, Canada, May 2017.

MacCannell, A.D.V., Sinclair, K.J., Friesen-Waldner L.J., McKenzie C.A., and Staples, J.F. WTF: What's This Fat? Identification of Eye Fat Deposit Discovered by Water-Fat MRI in Hibernating Squirrels. Oral presentation delivered at the Canadian Society of Zoologists conference, Winnipeg MB, Canada, May 2017.

MacCannell, A.D.V., Sinclair, K.J., Friesen-Waldner L.J., McKenzie C.A., and Staples, J.F. Water-fat MRI demonstrates seasonal proliferation of brown adipose tissue near the eyes of juvenile hibernators: An additive effect of cold exposure. Electronic Poster delivered at the International Society for Magnetic Resonance in Medicine, Honolulu HI, April 2017.

MacCannell, A.D.V., Sinclair, K.J., Friesen-Waldner L.J., McKenzie C.A., and Staples, J.F. Water-Fat MRI Reveals Growth of Brown Adipose Tissue Without Cold Exposure in a Hibernator. Poster presentation delivered at the Fallona Family Interdisciplinary research day, London, ON Canada, December 2017.

MacCannell, A.D.V., Sinclair, K.J., Friesen-Waldner L.J., McKenzie C.A., and Staples, J.F. Water-Fat MRI Suggests an Endogenous Rhythm of Brown Adipose Tissue Proliferation in a Hibernator. Oral presentation delivered at the Biology Graduate Research Forum, London, ON Canada, October 2016.

PUBLICATIONS

MacCannell, A.D.V., Jackson, E.C., Mathers, K.E., and Staples, J.F. An Improved Method for Detecting Torpor Entrance and Arousal in a Mammalian Hibernator Using Heart Rate Data. J. Exp. Biol. 2018 Jan; Doi: 10.1242/jeb.174508.

MacCannell, A.D.V., Sinclair, K.J., Friesen-Waldner L.J., McKenzie C.A., and Staples, J.F. Water-Fat MRI Reveals Growth of Brown Adipose Tissue Without Cold Exposure in a Hibernator. J Comp Physiol [B] 2017 Jul; 187:759-767.